

---

# Pretraining Decision Transformers with Reward Prediction for In-Context Multi-task Structured Bandit Learning

---

**Subhojyoti Mukherjee**  
ECE Department  
UW-Madison  
Wisconsin, Madison  
smukherjee27@wisc.edu

Josiah P. Hanna  
CS Department  
UW-Madison  
Wisconsin, Madison

Qiaomin Xie  
ISyE Department  
UW-Madison  
Wisconsin, Madison

Robert Nowak  
ECE Department  
UW-Madison  
Wisconsin, Madison

## Abstract

In this paper, we study multi-task structured bandit problem where the goal is to learn a near-optimal algorithm that minimizes cumulative regret. The tasks share a common structure and the algorithm exploits the shared structure to minimize the cumulative regret for an unseen but related test task. We use a transformer as a decision-making algorithm to learn this shared structure so as to generalize to the test task. The prior work of pretrained decision transformers like **DPT** requires access to the optimal action during training which may be hard in several scenarios. Diverging from these works, our learning algorithm does not need the knowledge of optimal action per task during training but predicts a reward vector for each of the actions using only the observed offline data from the diverse training tasks. Finally, during inference time, it selects action using the reward predictions employing various exploration strategies in-context for an unseen test task. We show that our model outperforms other SOTA methods like **DPT**, and Algorithmic Distillation (**AD**) over a series of experiments on several structured bandit problems (linear, bilinear, latent, non-linear). Interestingly, we show that our algorithm, without the knowledge of the underlying problem structure, can learn a near-optimal policy in-context by leveraging the shared structure across diverse tasks. We further extend the field of pre-trained decision transformers by showing that they can leverage unseen tasks with new actions and still learn the underlying latent structure to derive a near-optimal policy. We validate this over several experiments to show that our proposed solution is very general and has wide applications to potentially emergent online and offline strategies at test time. Finally, we theoretically analyze the performance of our algorithm and obtain generalization bounds in the in-context multi-task learning setting.

## 1 Introduction

In this paper, we study multi-task bandit learning with the goal of learning an algorithm that discovers and exploits structure in a family of related tasks. In multi-task bandit learning, we have multiple distinct bandit tasks for which we want to learn a policy. Though distinct, the tasks share some structure, which we hope to leverage to speed up learning on new instances in this task family. Traditionally, the study of such structured bandit problems has relied on knowledge of the problem structure like linear bandits [Li et al., 2010, Abbasi-Yadkori et al., 2011, Degenne et al., 2020],

bilinear bandits [Jun et al., 2019], hierarchical bandits [Hong et al., 2022a,b], Lipschitz bandits [Bubeck et al., 2008, 2011, Magureanu et al., 2014], other structured bandits settings [Riquelme et al., 2018, Lattimore and Szepesvári, 2019, Dong et al., 2021] and even linear and bilinear multi-task bandit settings [Yang et al., 2022a, Du et al., 2023, Mukherjee et al., 2023]. When structure is unknown an alternative is to adopt sophisticated model classes, such as kernel machines or neural networks, exemplified by kernel or neural bandits [Valko et al., 2013, Chowdhury and Gopalan, 2017, Zhou et al., 2020, Dai et al., 2022]. However, these approaches are also costly as they learn complex, nonlinear models from the ground up without any prior data [Justus et al., 2018, Zambaldi et al., 2018].

In this paper, we consider an alternative approach of synthesizing a bandit algorithm from historical data where the data comes from recorded bandit interactions with past instances of our target task family. Concretely, we are given a set of state-action-reward tuples obtained by running some bandit algorithm in various instances from the task family. We then aim to learn a transformer [Vaswani et al., 2017] from this data that can in-context learn on new task instances. Laskin et al. [2022] consider a similar goal and introduce the Algorithm Distillation (AD) method, however, AD aims to copy the algorithm used in the historical data and thus is limited by the ability of the data collection algorithm. Lee et al. [2023] develop an approach, DPT, that enables learning a transformer that obtains lower regret in-context bandit learning compared to the algorithm used to produce the historical data. However, this approach requires knowledge of the optimal action at each stage of the decision process. In real problems, this assumption is hard to satisfy and we will show that DPT performs poorly when the optimal action is only approximately known. With this past work in mind, the goal of this paper is to answer the question:

*Can we learn an in-context bandit learning algorithm that obtains lower regret than the algorithm used to produce training data without knowledge of optimal actions in each training task?*

To answer this question, we introduce a new transformer methodology that obviates the need for knowledge of the optimal action in the in-context data — a piece of information that is often inaccessible. Our key observation is that while the mean rewards of each action change from task to task, certain probabilistic dependencies are persistent across all tasks with a given structure [Yang et al., 2020, 2022a, Mukherjee et al., 2023]. These probabilistic dependencies can be learned from the pretraining data and exploited to better estimate mean rewards and improve performance in a new unknown test task. The nature of the probabilistic dependencies depends on the specific structure of the bandit and can be complex (i.e., higher-order dependencies beyond simple correlations). We propose to use transformer models as a general-purpose architecture to capture the unknown dependencies by training transformers to predict the mean rewards in each of the given trajectories [Mirchandani et al., 2023, Zhao et al., 2023]. The key idea is that transformers have the capacity to discover and exploit complex dependencies in order to predict the rewards of all possible actions in each task from a *small* history of action-reward pairs in a new task. This paper demonstrates how such an approach can achieve state-of-the-art performance, relying solely on historical data, without the need for any supplementary information like the action features or knowledge of the complex reward models. Our new decision transformer learns to adapt, in-context, to novel actions as well as new tasks.

## Contributions

1. We introduce a new training procedure where predicting the next reward for all arms circumvents the issue of requiring access to the optimal (or approximately optimal) action during training time.
2. We demonstrate empirically that this training procedure results in lower regret in a wide series of tasks (such as linear, nonlinear, bilinear, and latent bandits) compared to **DPT**, **AD** (and other in-context decision-making algorithms).
3. We also show that our training procedure leverages the latent structure even when new actions are introduced both during training and testing time.
4. Finally, we theoretically analyze the generalization ability of **PreDeToR** through the lens of algorithmic stability and new results for the transformer setting.

## 2 Background

In this section, we first introduce our notation and the multi-task, structured bandit setting. We then formalize the in-context learning model studied in [Laskin et al. \[2022\]](#), [Lee et al. \[2023\]](#), [Sinii et al. \[2023\]](#), [Lin et al. \[2023\]](#), [Ma et al. \[2023\]](#), [Liu et al. \[2023c,a\]](#). We choose [DPT \[Lee et al., 2023\]](#) as a representative example of this learning model and explain the [DPT](#) model for the online setting.

### 2.1 Preliminaries

In this paper, we consider the multi-task linear bandit setting [[Du et al., 2023](#), [Yang et al., 2020](#), [2022a](#)]. In the multi-task setting, we denote each task as  $m$ . Each task  $m$  constitutes of the action set  $|\mathcal{A}| = A$  and the feature space  $\mathcal{X}$ . The actions in  $\mathcal{A}$  are indexed by  $a = 1, 2, \dots, A$ . The feature of each action is denoted by  $\mathbf{x}(m, a) \in \mathbb{R}^d$  and  $d \ll A$ . Denote  $\Delta(\mathcal{A})$  as the probability simplex over the action space  $\mathcal{A}$ . We denote a policy as  $\pi : \mathcal{A} \rightarrow [0, 1]$ , as a probability distribution over actions such that  $\pi \in \Delta(\mathcal{A})$ . This implies that  $\sum_{a=1}^A \pi(a) = 1$ .

Define  $[n] = \{1, 2, \dots, n\}$ . In a multi-task structured bandit setting the expected reward for each action in each task is assumed to be an unknown function of the hidden parameter and action features [[Lattimore and Szepesvári, 2020](#), [Gupta et al., 2020](#)]. The interaction proceeds iteratively over  $n$  rounds for each task  $m \in [M]$ . At each round  $t \in [n]$  for each task  $m \in [M]$ , the learner selects an action  $I_{m,t} \in \mathcal{A}$  and observes the reward  $r_{m,t} = f(\mathbf{x}(I_{m,t}), \boldsymbol{\theta}_{m,*}) + \eta_{m,t}$ , where  $\boldsymbol{\theta}_{m,*} \in \mathbb{R}^d$  is the hidden parameter specific to the task  $m$  to be learned by the learner. The function  $f(\cdot, \cdot)$  is the unknown reward structure. This can be  $f(\mathbf{x}(I_{m,t}), \boldsymbol{\theta}_{m,*}) = \mathbf{x}(I_{m,t})^\top \boldsymbol{\theta}_{m,*}$  for the linear setting or even more complex correlation between features and  $\boldsymbol{\theta}_{m,*}$  [[Filippi et al., 2010](#), [Abbasi-Yadkori et al., 2011](#), [Riquelme et al., 2018](#), [Lattimore and Szepesvári, 2019](#), [Dong et al., 2021](#)]. We further assume that the noise  $\eta_{m,t}$  is  $\sigma^2$  sub-Gaussian.

In our paper, we assume that there exist weak demonstrators denoted by  $\pi^w$ . These weak demonstrators are stochastic  $A$ -armed bandit algorithms like Upper Confidence Bound (UCB) [[Auer et al., 2002](#), [Auer and Ortner, 2010](#)] or Thompson Sampling [[Thompson, 1933](#), [Agrawal and Goyal, 2012](#), [Russo et al., 2018](#), [Zhu and Tan, 2020](#)]. The  $\pi^w$  at every round  $t$  for a task  $m \in [M]$  samples an action  $I_{m,t}$  and observes the reward  $r_{m,t} = f(\mathbf{x}(I_{m,t}), \boldsymbol{\theta}_{m,*}) + \eta_{m,t}$ . Crucially note that  $\pi^w$  does not observe the feature  $\mathbf{x}(I_{m,t})$ . Moreover, we assume that the  $\pi^w$  does not have access to the feature space  $\mathcal{X}$  for any task  $m$ , and hence cannot plan its sampling policy based on the feature vectors. The  $\pi^w$  is used to collect data on which we train our model. So we call these algorithms weak demonstrators. Note that in many real-world world settings, like robotics [[Fong et al., 2003](#), [Lauri et al., 2022](#)], medical treatment [[Murphy, 2003](#)] the task is only partially observed or have a complex correlated structure and therefore a learning agent may not have access to the full set of action features, but only observe the reward and action history. This is characterized by  $\pi^w$ . In the next section, we propose the learning model for the training procedure.

### 2.2 In-Context Learning Model

Similar to [Lee et al. \[2023\]](#), [Sinii et al. \[2023\]](#), [Lin et al. \[2023\]](#), [Ma et al. \[2023\]](#), [Liu et al. \[2023c,a\]](#) we assume the in-context learning model. We first discuss the pretraining procedure.

**Pretraining:** Let  $\mathcal{T}_{\text{pre}}$  denote the distribution over tasks  $m$  at the time of pretraining. Note that by our definition of the task  $m$ , the distribution  $\mathcal{T}_{\text{pre}}$  can span different reward and action spaces. Let  $\mathcal{D}_{\text{pre}}$  be the distribution over all possible interactions that the  $\pi^w$  can generate. We first sample a task  $m \sim \mathcal{T}_{\text{pre}}$  and then a context (or a prompt)  $\mathcal{H}_m$  which is a sequence of interactions for  $n$  rounds conditioned on the task  $m$  such that  $\mathcal{H}_m \sim \mathcal{D}_{\text{pre}}(\cdot|m)$ . So  $\mathcal{H}_m = \{I_{m,t}, r_{m,t}\}_{t=1}^n$ . We call this dataset  $\mathcal{H}_m$  an in-context dataset as it contains the contextual information about the task  $m$ . We denote the samples in  $\mathcal{H}_m$  till round  $t$  as  $\mathcal{H}_m^t = \{I_{m,s}, r_{m,s}\}_{s=1}^{t-1}$ . This dataset  $\mathcal{H}_m$  can be collected in several ways: (1) random interactions within  $m$ , (2) demonstrations from an expert, and (3) rollouts of an algorithm. Finally, we train a causal GPT-2 transformer model TF parameterized by  $\Theta$  on this dataset  $\mathcal{D}_{\text{pre}}$ . Specifically, we define  $\text{TF}_\Theta(\cdot | \mathcal{H}_m^t)$  as the transformer model that observes the dataset  $\mathcal{H}_m^t$  till round  $t$  and then produces a distribution over the actions. Our primary novelty lies in our training procedure which we explain in detail in [Section 3.1](#).

**Testing:** We now discuss the testing procedure for our setting. Let  $\mathcal{T}_{\text{test}}$  denote the distribution over test tasks  $m \in [M_{\text{test}}]$  at the time of testing. Let  $\mathcal{D}_{\text{test}}$  denote a distribution over all possible interactions that can be generated by  $\pi^w$  during test time. For online training, the dataset  $\mathcal{H}_m = \{\emptyset\}$  is initialized

empty. At each round  $t$ ,  $\text{TF}_{\Theta}(\cdot | \mathcal{H}_m^t)$  is deployed where the model samples  $I_t \sim \text{TF}_{\Theta}(\cdot | \mathcal{H}_m^t)$ . The model observes the reward  $r_t$  which is added to  $\mathcal{H}_m^t$ . So the  $\mathcal{H}_m$  during online testing consists of  $\{I_t, r_t\}_{t=1}^n$  collected during testing. This interaction procedure is conducted for each test task  $m \in [M_{\text{test}}]$ . Finally, note that in this testing phase, the model parameter  $\Theta$  is not updated. Finally, the goal of the learner is to minimize cumulative regret for all task  $m \in [M_{\text{test}}]$  defined as follows:  $\mathbb{E}[R_n] = \frac{1}{M_{\text{test}}} \sum_{m=1}^{M_{\text{test}}} \sum_{t=1}^n \max_{a \in \mathcal{A}} f(\mathbf{x}(m, a) - \mathbf{x}(m, I_t), \theta_{m,*})$ .

### 2.3 Related In-context Learning Algorithms

In this section, we discuss related algorithms for in-context decision-making. For completeness, we describe the **DPT** and **AD** training procedure and algorithm now. During training, **DPT** first samples  $m \sim \mathcal{T}_{\text{pre}}$  and then an in-context dataset  $\mathcal{H}_m \sim \mathcal{D}_{\text{pre}}(\cdot, m)$ . It adds this  $\mathcal{H}_m$  to the training dataset  $\mathcal{H}_{\text{train}}$ , and repeats to collect  $M_{\text{pre}}$  such training tasks. For each task  $m$ , **DPT** requires the optimal action  $a_{m,*} = \arg \max_a f(\mathbf{x}(m, a), \theta_{m,*})$  where  $f(\mathbf{x}(m, a), \theta_{m,*})$  is the expected reward for the action  $a$  in task  $m$ . Since the optimal action is usually not known in advance, in Section 4 we introduce a practical variant of **DPT** that approximates the optimal action with the best action identified during task interaction. During training **DPT** minimizes the cross-entropy loss:

$$\mathcal{L}_t^{\text{DPT}} = \text{cross-entropy}(\text{TF}_{\Theta}(\cdot | \mathcal{H}_m^t), p(a_{m,*})) \quad (1)$$

where  $p(a_{m,*}) \in \Delta^A$  is a one-hot vector such that  $p(j) = 1$  when  $j = a_{m,*}$  and 0 otherwise. This loss is then back-propagated and used to update the model parameter  $\Theta$ .

During test time evaluation for online setting the **DPT** selects  $I_t \sim \text{softmax}_a^\tau(\text{TF}_{\Theta}(\cdot | \mathcal{H}_m^t))$  where we define the  $\text{softmax}_a^\tau(\mathbf{v})$  over a  $A$  dimensional vector  $\mathbf{v} \in \mathbb{R}^A$  as  $\text{softmax}_a^\tau(\mathbf{v}(a)) = \exp(\mathbf{v}(a)/\tau) / \sum_{a'=1}^A \exp(\mathbf{v}(a')/\tau)$  which produces a distribution over actions weighted by the temperature parameter  $\tau > 0$ . Therefore this sampling procedure has a high probability of choosing the predicted optimal action as well as induce sufficient exploration. In the online setting, the **DPT** observes the reward  $r_t(I_t)$  which is added to  $\mathcal{H}_m^t$ . So the  $\mathcal{H}_m$  during online testing consists of  $\{I_t, r_t\}_{t=1}^n$  collected during testing. This interaction procedure is conducted for each test task  $m \in [M_{\text{test}}]$ . In the testing phase, the model parameter  $\Theta$  is not updated.

An alternative to **DPT** that does *not* require knowledge of the optimal action is the **AD** approach [Laskin et al., 2022, Lu et al., 2023]. In **AD**, the learner aims to predict the next action of the demonstrator. So it minimizes the cross-entropy loss as follows:

$$\mathcal{L}_t^{\text{AD}} = \text{cross-entropy}(\text{TF}_{\Theta}(\cdot | \mathcal{H}_m^t), p(I_{m,t})) \quad (2)$$

where  $p(I_{m,t})$  is a one-hot vector such that  $p(j) = 1$  when  $j = I_{m,t}$  (the true action taken by the demonstrator) and 0 otherwise. During online test time evaluation the **AD** selects  $I_t \sim \text{softmax}_a^\tau(\text{TF}_{\Theta}(\cdot | \mathcal{H}_m^t))$ . Unfortunately, **AD** will, at best, match the regret of the demonstrator and cannot obtain lower regret. In the next section, we introduce a new method that can improve upon the demonstrator without knowledge of the optimal action.

## 3 Proposed Algorithm PreDeToR

We now introduce our main algorithmic contribution, **PreDeToR**, which does not require access to the optimal action during training in order to improve upon the demonstrator.

### 3.1 Follow Demonstrator and Predict Next Reward

The key idea behind **DPT** is to leverage the in-context learning ability of transformers to infer the reward of each arm in a given test task. By training this in-context ability on a set of training tasks, the transformer can implicitly learn structure in the task family and exploit this structure to infer rewards without trying every single arm. Thus, in contrast to **DPT** and **AD** that output actions direction, **PreDeToR** outputs a scalar value reward prediction for each arm. To this effect, we append a linear layer of dimension  $A$  on top of a causal GPT2 model, denoted by  $\text{TF}^r_{\Theta}(\cdot | \mathcal{H}_m)$ , and use an MSE loss to train the transformer to predict the reward for each action with these outputs. Note that we use  $\text{TF}^r_{\Theta}(\cdot | \mathcal{H}_m)$  to denote a reward prediction transformer and  $\text{TF}_{\Theta}(\cdot | \mathcal{H}_m)$  as the transformer that predicts a distribution over actions (as in **DPT** and **AD**). Recall that the dataset  $\mathcal{H}_m \sim \mathcal{D}_{\text{pre}}(\cdot, m)$  where  $m \sim \mathcal{T}_{\text{pre}}$ . Note that dataset consists of a history of interactions  $\mathcal{H}_m = \{I_{m,t}, r_{m,t}\}_{t=1}^n$ . Then we pass this dataset to the transformer  $\text{TF}^r_{\Theta}(\cdot | \mathcal{H}_m)$ . At every round  $t$  the transformer predicts the *next reward* for each of the actions  $a \in \mathcal{A}$  for the task  $m$  based on  $\mathcal{H}_m^t = \{I_{m,s}, r_{m,s}\}_{s=1}^{t-1}$ . This predicted reward is denoted by  $\hat{r}_{m,t+1}(a)$  for each  $a \in \mathcal{A}$ .

**Loss calculation:** For each training task,  $m$ , we calculate the loss at each round,  $t$ , using the transformer’s prediction  $\hat{r}_{m,t}(I_{m,t})$  and the actual observed reward  $r_{m,t}$  that followed action  $I_{m,t}$ . We use a least-squares loss function:

$$\mathcal{L}_t = (\hat{r}_{m,t}(I_{m,t}) - r_{m,t})^2 \quad (3)$$

and hence minimizing this loss will minimize the mean squared-error of the transformer’s predictions. The loss is calculated using (3) and is backpropagated to update the model parameter  $\Theta$ .

**Exploratory Demonstrator:** Observe from the loss definition in (3) that it is calculated from the observed true reward and action from the dataset  $\mathcal{H}_m$ . In order for the transformer to learn accurate reward predictions during training, we require that the weak demonstrator is sufficiently exploratory such that it collects  $\mathcal{H}_m$  such that  $\mathcal{H}_m$  contains some reward  $r_{m,t}$  for each action  $a$ . We discuss in detail the impact of the demonstrator on **PreDeToR** ( $-\tau$ ) training in Appendix A.13.

### 3.2 Deploying **PreDeToR** for the online setting

In this section, we present the entire pseudocode of our algorithm and discuss how it is deployed for online setting. In the online setting, **PreDeToR**, first chooses the task  $m \sim \mathcal{T}_{\text{test}}$ , and the training dataset  $\mathcal{H}_m$  is initialized empty. Then at every round  $t$ , **PreDeToR** chooses  $I_t = \arg \max_{a \in \mathcal{A}} \text{TF}^r_{\Theta}(\hat{r}_{m,t}(a) \mid \mathcal{H}_m^t)$  which is the action with the highest predicted reward and  $\hat{r}_{m,t}(a)$  is the predicted reward of action  $a$ . Note that **PreDeToR** is a greedy policy and may not conduct sufficient exploration. Therefore we also introduce a soft variant, **PreDeToR** $-\tau$  that chooses  $I_t \sim \text{softmax}_a^{\tau}(\text{TF}^r_{\Theta}(\hat{r}_{m,t}(a) \mid \mathcal{H}_m^t))$ . Note that **PreDeToR** now adds the observed reward  $r_t(I_t)$  at round  $t$  to the dataset  $\mathcal{H}_m$  and then uses that to act greedily for the next round  $t + 1$ . The full pseudocode of **PreDeToR** in the online setting is in Algorithm 1. We discuss how **PreDeToR** ( $-\tau$ ) is deployed in the offline setting in Appendix A.15.

---

#### Algorithm 1 Pre-trained Decision Transformer with Reward Estimation (**PreDeToR**)

---

- 1: **Collecting Pretraining Dataset**
  - 2: Initialize empty pretraining dataset  $\mathcal{H}_{\text{train}}$
  - 3: **for**  $i$  in  $[M_{\text{pre}}]$  **do**
  - 4:   Sample task  $m \sim \mathcal{T}_{\text{pre}}$ , in-context dataset  $\mathcal{H}_m \sim \mathcal{D}_{\text{pre}}(\cdot \mid m)$  and add this to  $\mathcal{H}_{\text{train}}$ .
  - 5: **end for**
  - 6: **Pretraining model on dataset**
  - 7: Initialize model  $\text{TF}^r_{\Theta}$  with parameters  $\Theta$
  - 8: **while** not converged **do**
  - 9:   Sample  $\mathcal{H}_m$  from  $\mathcal{H}_{\text{train}}$  and predict  $\hat{r}_{m,t}$  for action  $(I_{m,t})$  for all  $t \in [n]$
  - 10:   Compute loss in (3) with respect to  $r_{m,t}$  and backpropagate to update model parameter  $\Theta$ .
  - 11: **end while**
  - 12: **Online test-time deployment**
  - 13: Sample unknown task  $m \sim \mathcal{T}_{\text{test}}$  and initialize empty  $\mathcal{H}_m^0 = \{\emptyset\}$
  - 14: **for**  $t = 1, 2, \dots, n$  **do**
  - 15:   Use  $\text{TF}^r_{\Theta}$  on  $m$  at round  $t$  to choose
 
$$I_t \begin{cases} = \arg \max_{a \in \mathcal{A}} \text{TF}^r_{\Theta}(\hat{r}_{m,t}(a) \mid \mathcal{H}_m^t), & \text{PreDeToR} \\ \sim \text{softmax}_a^{\tau} \text{TF}^r_{\Theta}(\hat{r}_{m,t}(a) \mid \mathcal{H}_m^t), & \text{PreDeToR-}\tau \end{cases}$$
  - 16:   Add  $\{I_t, r_t\}$  to  $\mathcal{H}_m^t$
  - 17: **end for**
- 

## 4 Empirical Study: Low Data Regime

In this section, we show that **PreDeToR** achieves lower regret than other in-context algorithms for the low data regime. In a low data regime, every task has a short horizon  $n$  which makes this a challenging setup as there is less data available per task. Therefore any good learner must learn to leverage the structure across the tasks. This setting is quite common in recommender settings where a user interaction with the system lasts only for a few rounds [Kwon et al., 2022, Tomkins et al., 2020]. We also analyze the exploration strategy of **PreDeToR** ( $-\tau$ ) in this setting. We study the performance of **PreDeToR** in the large horizon setting in Appendix A.7.

**Baselines:** We first discuss the baselines used in this setting.

- (1) **PreDeToR:** This is our proposed method shown in Algorithm 1.
- (2) **PreDeToR- $\tau$ :** This is the proposed exploratory method shown in Algorithm 1 and we fix  $\tau = 0.05$ .
- (3) **DPT-greedy:** This baseline is the greedy approximation of the DPT algorithm from Lee et al. [2023] which is discussed in Section 2.3. Note that we choose DPT-greedy as a representative example of similar in-context decision-making algorithms studied in Lee et al. [2023], Siniĭ et al. [2023], Lin et al. [2023], Ma et al. [2023], Liu et al. [2023c,a] all of which require the optimal action (or its greedy approximation). We choose DPT as a representative example of this learning procedure. The DPT-greedy uses training data  $\mathcal{H}_{\text{train}}$  to estimate the optimal action for each task  $m$ . For each task  $m$ , it DPT-greedy evaluates the optimal action  $\hat{a}_{m,*} = \arg \max_a \sum_{t=1}^n \hat{r}_{m,t}(a)$  where,  $\hat{r}_{m,t}(a) = \sum_{s=1}^n \hat{r}_{m,t} \mathbf{1}(I_s = a)$  is the observed cumulative reward for the action  $a$  in task  $m$  and  $\mathbf{1}(\cdot)$  is the indicator function. Note that the optimal action  $\hat{a}_{m,*}$  is evaluated using the entire dataset  $\mathcal{H}_m$ . Finally, it implements the training procedure as discussed in Section 2.3.
- (4) **AD:** This is the Algorithmic Distillation method [Laskin et al., 2022, Lu et al., 2021] discussed in Section 2.3.
- (5) **Thomp:** This baseline is the stochastic  $A$ -actioned bandit Thompson Sampling algorithm from Thompson [1933], Agrawal and Goyal [2012], Russo et al. [2018], Zhu and Tan [2020]. We briefly describe the algorithm below: At every round  $t$  and each action  $a$ , Thomp samples  $\gamma_{m,t}(a) \sim \mathcal{N}(\hat{\mu}_{m,t-1}(a), \sigma^2/N_{m,t-1}(a))$ , where  $N_{m,t-1}(a)$  is the number of times the action  $a$  has been selected till  $t-1$ , and  $\hat{\mu}_{m,t-1}(a) = \frac{\sum_{s=1}^{t-1} \hat{r}_{m,s} \mathbf{1}(I_s = a)}{N_{m,t-1}(a)}$  is the empirical mean. Then the action selected at round  $t$  is  $I_t = \arg \max_a \gamma_{m,t}(a)$ . Observe that Thomp is not a deterministic algorithm like UCB [Auer et al., 2002]. So we choose Thomp as the weak demonstrator  $\pi^w$  because it is more exploratory than UCB and also chooses the optimal action  $a_{m,*}$  sufficiently large number of times. Thomp is a weak demonstrator as it does not have access to the feature set  $\mathcal{X}$  for any task  $m$ .
- (6) **LinUCB:** (Linear Upper Confidence Bound): This baseline is the Upper Confidence Bound algorithm for the linear bandit setting that selects the action  $I_t$  at round  $t$  for task  $m$  that is most optimistic and reduces the uncertainty of the task unknown parameter  $\theta_{m,*}$ . To balance exploitation and exploration between choosing different items the LinUCB computes an upper confidence value to the estimated mean of each action  $\mathbf{x}_{m,a} \in \mathcal{X}$ . This is done as follows: At every round  $t$  for task  $m$ , it calculates the ucb value  $B_{m,a,t}$  for each action  $\mathbf{x}_{m,a} \in \mathcal{X}$  such that  $B_{m,a,t} = \mathbf{x}_{m,a}^\top \hat{\theta}_{m,t-1} + \alpha \|\mathbf{x}_{m,a}\|_{\Sigma_{m,t-1}^{-1}}$  where  $\alpha > 0$  is a constant and  $\hat{\theta}_{m,t}$  is the estimate of the model parameter  $\theta_{m,*}$  at round  $t$ . Here,  $\Sigma_{m,t-1} = \sum_{s=1}^{t-1} \mathbf{x}_{m,s} \mathbf{x}_{m,s}^\top + \lambda \mathbf{I}_d$  is the data covariance matrix or the arms already tried. Then it chooses  $I_t = \arg \max_a B_{m,a,t}$ . Note that LinUCB is a strong demonstrator that we give oracle access to the features of each action; other algorithms do not observe the features. Hence, in linear bandits, LinUCB provides an approximate upper bound on the performance of all algorithms.

**Outcomes:** Before presenting the result we discuss the main outcomes from our experimental results in this section:

- (1) **PreDeToR (- $\tau$ )** learns to exploit the latent structure of the underlying tasks even when it is trained without the optimal action  $a_{m,*}$  (or its approximation) and without the action features  $\mathcal{X}$ .
- (2) **PreDeToR (- $\tau$ )** learns to exploit the reward correlation between tasks and is able to have an accurate reward estimate of the optimal action for each task  $m$ .
- (3) **PreDeToR (- $\tau$ )** outperforms its weak demonstrator even when it is trained without the optimal action  $a_{m,*}$  and without the feature set  $\mathcal{X}$ .

**Experimental Result:** These findings are reported in Figure 1. In Figure 1(a) we show the linear bandit setting for horizon  $n = 25$ ,  $M_{\text{pre}} = 200000$ ,  $M_{\text{test}} = 200$ ,  $A = 10$ , and  $d = 2$ . Further empirical setting details are stated in Appendix A.2. The demonstrator  $\pi^w$  is the Thomp algorithm. We observe that PreDeToR (- $\tau$ ) has lower cumulative regret than DPT-greedy, and AD. Note that for this low data regime the DPT-greedy does not have a good estimation of  $\hat{a}_{m,*}$  which results in a poor prediction of optimal action  $\hat{a}_{m,t,*}$ . This results in higher regret. Observe that PreDeToR (- $\tau$ ) performs quite similarly to LinUCB and lowers regret compared to Thomp which also shows that PreDeToR is able to exploit the latent linear structure and reward correlation of the underlying

tasks. **AD** is not able to outperform its demonstrator **Thomp** as it is trained to predict the next action of the demonstrator. In Figure 1(b) we show the non-linear bandit setting for horizon  $n = 50$ ,  $M_{\text{pre}} = 100000$ ,  $M_{\text{test}} = 200$ ,  $A = 6$ , and  $d = 2$ . The demonstrator  $\pi^w$  is the **Thomp** algorithm. Again we observe that **PreDeToR** ( $-\tau$ ) has lower cumulative regret than **DPT-greedy**. Note that **PreDeToR** ( $-\tau$ ) has lower regret than **LinUCB** which fails to perform well in this non-linear setting due to its algorithmic design. Finally, **PreDeToR** ( $-\tau$ ) performs slightly better than **PreDeToR** in both settings as it conducts more exploration.

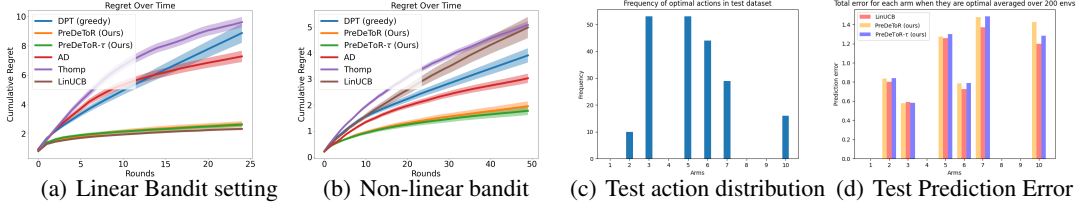


Figure 1: Low-Data regime. The horizontal axis is the number of rounds. Confidence bars show one standard error.

We also show how the prediction error of the optimal action by **PreDeToR** is small compared to **LinUCB** in the linear bandit setting. In Figure 1(c) we first show how the 10 actions are distributed in the  $M_{\text{test}} = 200$  test tasks. In Figure 1(c) for each bar, the frequency indicates the number of tasks where the action (shown in the x-axis) is the optimal action. Then, in Figure 1(d), we show the prediction error of **PreDeToR** ( $-\tau$ ) for each task  $m \in [M_{\text{test}}]$ . The prediction error is calculated as  $(\hat{\mu}_{m,n,*}(a) - \mu_{m,*}(a))^2$  where  $\hat{\mu}_{m,n,*}(a) = \max_a \hat{\theta}_{m,n}^\top \mathbf{x}_m(a)$  is the empirical mean at the end of round  $n$ , and  $\mu_{*,m}(a) = \max_a \theta_{*,m}^\top \mathbf{x}_m(a)$  is the true mean of the optimal action in task  $m$ . Then we average the prediction error for the action  $a \in [A]$  by the number of times the action  $a$  is the optimal action in some task  $m$ . From the Figure 1(d), we see that for actions  $\{2, 3, 5, 6, 7, 10\}$ , the prediction error of **PreDeToR** is either close or smaller than **LinUCB**. Note that **LinUCB** estimates the empirical mean directly from the test task, whereas **PreDeToR** has a strong prior based on the training data. So **PreDeToR** is able to estimate the reward of the optimal action quite well from the training dataset  $\mathcal{D}_{\text{pre}}$ . This shows the power of **PreDeToR** to go beyond the in-context decision-making setting studied in Lee et al. [2023], Lin et al. [2023], Ma et al. [2023], Sini et al. [2023], Liu et al. [2023c] which require long horizons/trajectories and optimal action during training to learn a near-optimal policy. We discuss how exploration of **PreDeToR** ( $-\tau$ ) results in low cumulative regret in Appendix A.11. Importantly, we show that predicting the reward has significant advantages in a low-data regime as it leads to the right notion of exploration.

## 5 Empirical Study: New Actions

In this section, we discuss how new actions introduced both during test time and data collection influence the performance of **PreDeToR** ( $-\tau$ ) and other baselines. These experiments go beyond what is studied in Lee et al. [2023], Lin et al. [2023], Ma et al. [2023], Liu et al. [2023c] as they only study the performance in setting when  $\mathcal{D}_{\text{test}} = \mathcal{D}_{\text{pre}}$ . Moreover, these experiments are particularly important as they show the extent to which **PreDeToR** ( $-\tau$ ) is leveraging the latent structure.

**Invariant actions:** We denote the set of actions fixed across the different tasks in the pretraining in-context dataset as  $\mathcal{A}^{\text{inv}}$ . Therefore these action features  $\mathbf{x}(a) \in \mathbb{R}^d$  for  $a \in \mathcal{A}^{\text{inv}}$  are fixed across the different tasks  $m$ . Note that these invariant actions help the transformer  $\text{TF}_w$  to learn the latent structure and the reward correlation across the different tasks.

**New actions:** However, we also want to test how robust is **PreDeToR** ( $-\tau$ ) to new actions not seen during training time. To this effect, for each task  $m \in [M_{\text{pre}}]$  and  $m \in [M_{\text{test}}]$  we introduce  $A - |\mathcal{A}^{\text{inv}}|$  new actions. For each of these new actions  $a \in [A - |\mathcal{A}^{\text{inv}}|]$  we choose the features  $\mathbf{x}(m, a)$  randomly from  $\mathcal{X} \subseteq \mathbb{R}^d$ . Note the transformer now trains on a dataset  $\mathcal{H}_m \subseteq \mathcal{D}_{\text{pre}} \neq \mathcal{D}_{\text{test}}$ .

**Baselines:** We implement the same baselines discussed in Section 4.

**Outcomes:** Again before presenting the result we discuss the main outcomes from our experimental results of introducing new actions during data collection and evaluation:

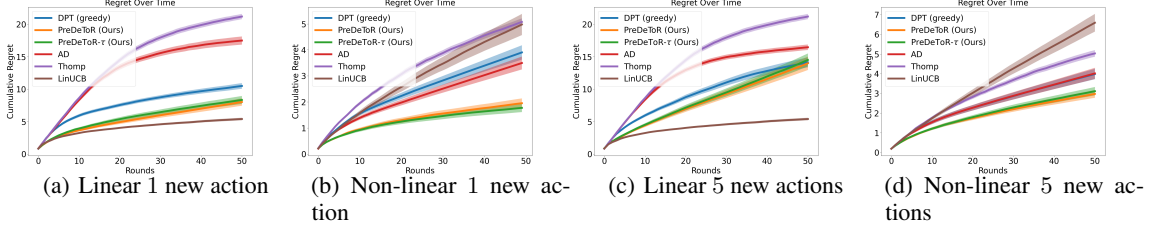


Figure 2: New action experiments. The horizontal axis is the number of rounds. Confidence bars show one standard error.

- (1) The **PreDeToR** ( $-\tau$ ) learns to exploit the underlying latent structure and reward correlation between the different tasks even when  $\mathcal{D}_{\text{test}} \neq \mathcal{D}_{\text{pre}}$  and the number of changing actions per task is small. So **PreDeToR** ( $-\tau$ ) is more robust to changing actions compared to **AD** and **DPT-greedy**.
- (2) **PreDeToR** ( $-\tau$ ) has lower regret than weak demonstrator even when it is trained on  $\mathcal{D}_{\text{pre}} \neq \mathcal{D}_{\text{test}}$ .
- (3) The **PreDeToR** ( $-\tau$ ) cumulative regret increases as the number of invariant actions decreases. This shows that invariant actions are important for learning the underlying latent structure and reward correlation across tasks.

**Experimental Result:** We observe these outcomes in Figure 2. We consider the linear bandit setting of horizon  $n = 50$ ,  $M_{\text{pre}} = 200000$ ,  $M_{\text{test}} = 200$ ,  $A = 20$ , and  $d = 5$ . Here during data collection and during collecting the test data, we randomly select one new action from  $\mathbb{R}^d$  for each task  $m$ . So the number of invariant actions is  $|\mathcal{A}^{\text{inv}}| = 19$ . Again, the demonstrator  $\pi^w$  is the **Thomp** algorithm. We observe that **PreDeToR** ( $-\tau$ ) has lower cumulative regret than **DPT-greedy**, and **AD**. The weak performance of **DPT-greedy** can be attributed to low data per task and inability to adapt when  $\mathcal{D}_{\text{pre}} \neq \mathcal{D}_{\text{test}}$ . Observe that **PreDeToR** ( $-\tau$ ) almost matches **LinUCB** and has lower regret than **Thomp**. This shows that **PreDeToR** ( $-\tau$ ) is able to exploit the latent linear structure of the underlying tasks. In Figure 2(b) we show the non-linear bandit setting for horizon  $n = 50$ ,  $M_{\text{pre}} = 100000$ ,  $M_{\text{test}} = 200$ ,  $A = 6$ ,  $d = 2$ , and  $|\mathcal{A}^{\text{inv}}| = 5$ . The demonstrator  $\pi^w$  is the **Thomp** algorithm. Again, we observe that **PreDeToR** has lower cumulative regret than **DPT-greedy** and **AD** and furthermore improves upon **LinUCB** which fails to perform well in this non-linear setting due to its assumption of linear rewards. **PreDeToR- $\tau$**  performs slightly better than **PreDeToR** in 1 new arm setting as it conducts more exploration.

In the following two experiments, we test the limit of robustness of **PreDeToR** ( $-\tau$ ) by decreasing the number of invariant actions. We use  $|\mathcal{A}^{\text{inv}}| = 15$  for linear, and  $|\mathcal{A}^{\text{inv}}| = 2$  for the non-linear setting. All the other task parameters are the same as in the previous two experiments. The corresponding results are shown in Figure 2(c) and Figure 2(d). Observe that in the linear setting (where **LinUCB** is effective), the performance of **PreDeToR** degrades compared to the case when  $|\mathcal{A}^{\text{inv}}| = 15$ . This shows that as the number of invariant actions decreases, the ability of **PreDeToR** ( $-\tau$ ) to estimate the underlying latent structure and reward correlation also decreases. In Appendix A.12, we analyze the exploration of **PreDeToR** ( $-\tau$ ) in this setting, which shows that the shared latent structure is essential for minimizing cumulative regret.

We also empirically study the test performance of **PreDeToR** ( $-\tau$ ) in other bandit settings such as bilinear bandits (Appendix A.3), latent bandits (Appendix A.4), draw a connection between **PreDeToR** and Bayesian estimators (Appendix A.5), and perform sensitivity and ablation studies in Appendix A.6, A.8, A.9, A.10. We discuss data collection algorithms in Appendix A.13 and the offline setting in Appendix A.15. Due to space constraints, we refer the interested reader to the relevant section in the appendices.

## 6 Theoretical Analysis

In this section, we present a theoretical analysis of how **PreDeToR- $\tau$**  generalizes to an unknown target task given a set of source tasks. We also show that in low-data regimes the **PreDeToR- $\tau$**  has a low expected excess risk for the unknown target task as the number of source tasks increases. We proceed as follows: Suppose we have the training data set  $\mathcal{H}_{\text{all}} = \{\mathcal{H}_m\}_{m=1}^{M_{\text{pre}}}$ , where the task  $m \sim \mathcal{T}$  with a distribution  $\mathcal{T}$  and the task data  $\mathcal{H}_m$  is generated from a distribution  $\mathcal{D}_{\text{pre}}(\cdot|m)$ . For illustration purposes, here we consider the training data distribution  $\mathcal{D}_{\text{pre}}(\cdot|m)$  where the actions are sampled following soft-LinUCB [Chu et al., 2011]. Note that soft-LinUCB produces a distribution over actions



(see Appendix A.14 for a detailed description). Given the loss function in (3), we can define the task  $m$  training loss of **PreDeToR- $\tau$**  as  $\widehat{\mathcal{L}}_m(\text{TF}^{\mathbf{r}_\Theta}) = \frac{1}{n} \sum_{t=1}^n \ell(r_{m,t}, \text{TF}^{\mathbf{r}_\Theta}(\widehat{r}_{m,t}(I_{m,t})|\mathcal{H}_m^t)) = \frac{1}{n} \sum_{t=1}^n (\text{TF}^{\mathbf{r}_\Theta}(\widehat{r}_{m,t}(I_{m,t})|\mathcal{H}_m^t) - r_{m,t})^2$ . We drop the notation  $\Theta, \mathbf{r}$  from  $\text{TF}^{\mathbf{r}_\Theta}$  for simplicity and let  $M = M_{\text{pre}}$ . We define

$$\widehat{\text{TF}} = \arg \min_{\text{TF} \in \text{Alg}} \widehat{\mathcal{L}}_{\mathcal{H}_{\text{all}}}(\text{TF}) := \frac{1}{M} \sum_{m=1}^M \widehat{\mathcal{L}}_m(\text{TF}), \quad (\text{ERM}) \quad (4)$$

where Alg denotes the space of algorithms induced by the TF. Let  $\mathcal{L}_m(\text{TF}) = \mathbb{E}_{\mathcal{H}_m}[\widehat{\mathcal{L}}_m(\text{TF})]$  and  $\mathcal{L}_{\text{MTL}}(\text{TF}) = \mathbb{E}[\widehat{\mathcal{L}}_{\mathcal{H}_{\text{all}}}(\text{TF})] = \frac{1}{M} \sum_{m=1}^M \mathcal{L}_m(\text{TF})$  be the corresponding population risks. For the ERM in (4), we want to bound the following excess Multi-Task Learning (MTL) risk of **PreDeToR- $\tau$**

$$\mathcal{R}_{\text{MTL}}(\widehat{\text{TF}}) = \mathcal{L}_{\text{MTL}}(\widehat{\text{TF}}) - \min_{\text{TF} \in \text{Alg}} \mathcal{L}_{\text{MTL}}(\text{TF}). \quad (5)$$

Note that in in-context learning, a training sample  $(I_t, r_t)$  impacts all future decisions of the algorithm from time step  $t + 1$  to  $n$ . Therefore, we need to control the stability of the input perturbation of the learning algorithm learned by the transformer. We introduce the following stability condition.

**Assumption 6.1.** (Error stability [Bousquet and Elisseeff, 2002, Li et al., 2023]). Let  $\mathcal{H} = (I_t, r_t)_{t=1}^n$  be a sequence in  $[A] \times [0, 1]$  with  $n \geq 1$  and  $\mathcal{H}'$  be the sequence where the  $t'$ th sample of  $\mathcal{H}$  is replaced by  $(I'_t, r'_t)$ . Error stability holds for a distribution  $(I, r) \sim \mathcal{D}$  if there exists a  $K > 0$  such that for any  $\mathcal{H}, (I'_t, r'_t) \in ([A] \times [0, 1]), t \leq n$ , and  $\text{TF} \in \text{Alg}$ , we have

$$|\mathbb{E}_{(I,r)} [\ell(r, \text{TF}(\widehat{r}(I)|\mathcal{H})) - \ell(r, \text{TF}(\widehat{r}(I)|\mathcal{H}')))]| \leq \frac{K}{n}$$

Let  $\rho$  be a distance metric on Alg. Pairwise error stability holds if for all  $\text{TF}, \text{TF}' \in \text{Alg}$  we have

$$|\mathbb{E}_{(x,y)} [\ell(r, \text{TF}(\widehat{r}(I)|\mathcal{H})) - \ell(r, \text{TF}'(\widehat{r}(I)|\mathcal{H})) - \ell(r, \text{TF}(\widehat{r}(I)|\mathcal{H}')) + \ell(r, \text{TF}'(\widehat{r}(I)|\mathcal{H}')))]| \leq \frac{K\rho(\text{TF}, \text{TF}')}{n}$$

Now we present the Multi-task learning (MTL) risk of **PreDeToR- $\tau$** .

**Theorem 6.2. (PreDeToR risk)** Suppose error stability Assumption 6.1 holds and assume loss function  $\ell(\cdot, \cdot)$  is  $C$ -Lipschitz for all  $r_t \in [0, B]$  and horizon  $n \geq 1$ . Let  $\widehat{\text{TF}}$  be the empirical solution of (ERM) and  $\mathcal{N}(\text{Alg}, \rho, \epsilon)$  be the covering number of the algorithm space Alg following Definition C.2 and C.3. Then with probability at least  $1 - 2\delta$ , the excess MTL risk of **PreDeToR- $\tau$**  is bounded by  $\mathcal{R}_{\text{MTL}}(\widehat{\text{TF}}) \leq 4\frac{C}{\sqrt{nM}} + 2(B + K \log n) \sqrt{\frac{\log(\mathcal{N}(\text{Alg}, \rho, \epsilon)/\delta)}{cnM}}$ , where  $\mathcal{N}(\text{Alg}, \rho, \epsilon)$  is the covering number of transformer  $\widehat{\text{TF}}$  and  $\epsilon = 1/\sqrt{nM}$ .

The proof of this theorem is provided in Appendix C.1. From Theorem 6.2 we see that in low-data regime with a small horizon  $n$ , as the number of tasks  $M$  increases the MTL risk decreases. We further discuss the stability factor  $K$  and covering number  $\mathcal{N}(\text{Alg}, \rho, \epsilon)$  in Remark C.4, and C.5.

We now present the transfer learning risk of **PreDeToR- $\tau$**  for an unknown target task  $g \sim \mathcal{T}$  with the test dataset  $\mathcal{H}_g \sim \mathcal{D}_{\text{test}}(\cdot|g)$ . Note that the test data distribution  $\mathcal{D}_{\text{test}}(\cdot|g)$  is such that the actions are sampled following soft-LinUCB.

**Theorem 6.3. (Transfer risk)** Consider the setting of Theorem 6.2 and assume the training source tasks are independently drawn from task distribution  $\mathcal{T}$ . Let  $\widehat{\text{TF}}$  be the empirical solution of (ERM) and  $g \sim \mathcal{T}$ . Define the expected excess transfer learning risk  $\mathbb{E}_g[\mathcal{R}_g] = \mathbb{E}_g[\mathcal{L}_g(\widehat{\text{TF}})] - \arg \min_{\text{TF} \in \text{Alg}} \mathbb{E}_g[\mathcal{L}_g(\text{TF})]$ . Then with probability at least  $1 - 2\delta$ , the  $\mathbb{E}_g[\mathcal{R}_g] \leq 4\frac{C}{\sqrt{M}} + 2B\sqrt{\frac{\log(\mathcal{N}(\text{Alg}, \rho, \epsilon)/\delta)}{M}}$ , where  $\mathcal{N}(\text{Alg}, \rho, \epsilon)$  is the covering number of  $\widehat{\text{TF}}$  and  $\epsilon = \frac{1}{\sqrt{M}}$ .

The proof is given in Appendix C.2. This shows that for the transfer learning risk of **PreDeToR- $\tau$**  (once trained on the  $M$  source tasks) scales with  $\tilde{O}(1/\sqrt{M})$ . This is because the unseen target task  $g \sim \mathcal{T}$  induces a distribution shift, which, typically, cannot be mitigated with more samples  $n$  per task. A similar observation is provided in Lin et al. [2023]. We further discuss this in Remark C.7. We also observe a similar phenomenon empirically; see the discussion in Appendix A.14.

## 7 Conclusions, Limitations and Future Works

In this paper, we studied the supervised pretraining of decision transformers in the multi-task structured bandit setting when the knowledge of the optimal action is unavailable. Moreover, our proposed methods **PreDeToR** ( $-\tau$ ) do not need to know the action representations or the reward structure and learn these in-context with the help of offline data. The **PreDeToR** ( $-\tau$ ) predict the reward for the next action of each action during pretraining and can generalize well in-context in several regimes spanning low-data, new actions, and structured bandit settings like linear, non-linear, bilinear, latent bandits. The **PreDeToR** ( $-\tau$ ) outperforms other in-context algorithms like **AD**, **DPT-greedy** in most of the experiments. Finally, we theoretically analyze **PreDeToR**- $\tau$  and show that pretraining it in  $M$  source tasks leads to a low expected excess error on a target task drawn from the same task distribution  $\mathcal{T}$ . In future, we want to extend our **PreDeToR** ( $-\tau$ ) to MDP setting [Sutton and Barto, 2018, Agarwal et al., 2019], and constraint MDP setting [Efroni et al., 2020, Gu et al., 2022].

## References

- Yasin Abbasi-Yadkori, Dávid Pál, and Csaba Szepesvári. Improved algorithms for linear stochastic bandits. *Advances in neural information processing systems*, 24, 2011.
- Alekh Agarwal, Nan Jiang, Sham M Kakade, and Wen Sun. Reinforcement learning: Theory and algorithms. *CS Dept., UW Seattle, Seattle, WA, USA, Tech. Rep.*, 32, 2019.
- Shipra Agrawal and Navin Goyal. Analysis of thompson sampling for the multi-armed bandit problem. In *Conference on learning theory*, pages 39–1. JMLR Workshop and Conference Proceedings, 2012.
- Peter Auer and Ronald Ortner. Ucb revisited: Improved regret bounds for the stochastic multi-armed bandit problem. *Periodica Mathematica Hungarica*, 61(1-2):55–65, 2010.
- Peter Auer, Nicolò Cesa-Bianchi, and Paul Fischer. Finite-time Analysis of the Multiarmed Bandit Problem. *Machine Learning*, 47(2):235–256, May 2002. ISSN 1573-0565. doi: 10.1023/A:1013689704352. URL <https://doi.org/10.1023/A:1013689704352>.
- Yoshua Bengio, Samy Bengio, and Jocelyn Cloutier. *Learning a synaptic learning rule*. Université de Montréal, Département d’informatique et de recherche . . . , 1990.
- C Bishop. Pattern recognition and machine learning. *Springer google schola*, 2:531–537, 2006.
- Olivier Bousquet and André Elisseeff. Stability and generalization. *The Journal of Machine Learning Research*, 2:499–526, 2002.
- George EP Box and George C Tiao. *Bayesian inference in statistical analysis*. John Wiley & Sons, 2011.
- David Brandfonbrener, Alberto Bietti, Jacob Buckman, Romain Laroché, and Joan Bruna. When does return-conditioned supervised learning work for offline reinforcement learning? *Advances in Neural Information Processing Systems*, 35:1542–1553, 2022.
- Anthony Brohan, Noah Brown, Justice Carbajal, Yevgen Chebotar, Joseph Dabis, Chelsea Finn, Keerthana Gopalakrishnan, Karol Hausman, Alex Herzog, Jasmine Hsu, et al. Rt-1: Robotics transformer for real-world control at scale. *arXiv preprint arXiv:2212.06817*, 2022.
- Sébastien Bubeck, Gilles Stoltz, Csaba Szepesvári, and Rémi Munos. Online optimization in x-armed bandits. *Advances in Neural Information Processing Systems*, 21, 2008.
- Sébastien Bubeck, Gilles Stoltz, and Jia Yuan Yu. Lipschitz bandits without the lipschitz constant. In *Algorithmic Learning Theory: 22nd International Conference, ALT 2011, Espoo, Finland, October 5-7, 2011. Proceedings 22*, pages 144–158. Springer, 2011.
- Bradley P Carlin and Thomas A Louis. *Bayesian methods for data analysis*. CRC press, 2008.
- Kamalika Chaudhuri, Prateek Jain, and Nagarajan Natarajan. Active heteroscedastic regression. In *International Conference on Machine Learning*, pages 694–702. PMLR, 2017.

- Lili Chen, Kevin Lu, Aravind Rajeswaran, Kimin Lee, Aditya Grover, Misha Laskin, Pieter Abbeel, Aravind Srinivas, and Igor Mordatch. Decision transformer: Reinforcement learning via sequence modeling. *Advances in neural information processing systems*, 34:15084–15097, 2021.
- Sayak Ray Chowdhury and Aditya Gopalan. On kernelized multi-armed bandits. In *International Conference on Machine Learning*, pages 844–853. PMLR, 2017.
- Wei Chu, Lihong Li, Lev Reyzin, and Robert Schapire. Contextual bandits with linear payoff functions. In *Proceedings of the Fourteenth International Conference on Artificial Intelligence and Statistics*, pages 208–214. JMLR Workshop and Conference Proceedings, 2011.
- Zhongxiang Dai, Yao Shu, Arun Verma, Flint Xiaofeng Fan, Bryan Kian Hsiang Low, and Patrick Jaillet. Federated neural bandit. *arXiv preprint arXiv:2205.14309*, 2022.
- Rémy Degenne, Pierre Ménard, Xuedong Shang, and Michal Valko. Gamification of pure exploration for linear bandits. In *International Conference on Machine Learning*, pages 2432–2442. PMLR, 2020.
- Kefan Dong, Jiaqi Yang, and Tengyu Ma. Provable model-based nonlinear bandit and reinforcement learning: Shelve optimism, embrace virtual curvature. *Advances in neural information processing systems*, 34:26168–26182, 2021.
- Yihan Du, Longbo Huang, and Wen Sun. Multi-task representation learning for pure exploration in linear bandits. *arXiv preprint arXiv:2302.04441*, 2023.
- Yan Duan, John Schulman, Xi Chen, Peter L Bartlett, Ilya Sutskever, and Pieter Abbeel. RL 2: Fast reinforcement learning via slow reinforcement learning. *arXiv preprint arXiv:1611.02779*, 2016.
- Yonathan Efroni, Shie Mannor, and Matteo Pirotta. Exploration-exploitation in constrained mdps. *arXiv preprint arXiv:2003.02189*, 2020.
- Valerii Vadimovich Fedorov. *Theory of optimal experiments*. Elsevier, 2013.
- Sarah Filippi, Olivier Cappé, Aurélien Garivier, and Csaba Szepesvári. Parametric bandits: The generalized linear case. *Advances in neural information processing systems*, 23, 2010.
- Chelsea Finn, Pieter Abbeel, and Sergey Levine. Model-agnostic meta-learning for fast adaptation of deep networks. In *International conference on machine learning*, pages 1126–1135. PMLR, 2017.
- Terrence Fong, Illah Nourbakhsh, and Kerstin Dautenhahn. A survey of socially interactive robots. *Robotics and autonomous systems*, 42(3-4):143–166, 2003.
- Vincent François-Lavet, Peter Henderson, Riashat Islam, Marc G Bellemare, Joelle Pineau, et al. An introduction to deep reinforcement learning. *Foundations and Trends® in Machine Learning*, 11(3-4):219–354, 2018.
- Justin Fu, Sergey Levine, and Pieter Abbeel. One-shot learning of manipulation skills with online dynamics adaptation and neural network priors. In *2016 IEEE/RSJ International Conference on Intelligent Robots and Systems (IROS)*, pages 4019–4026. IEEE, 2016.
- Scott Fujimoto, David Meger, and Doina Precup. Off-policy deep reinforcement learning without exploration. In *International conference on machine learning*, pages 2052–2062. PMLR, 2019.
- Yao Ge, Yuting Guo, Yuan-Chi Yang, Mohammed Ali Al-Garadi, and Abeed Sarker. Few-shot learning for medical text: A systematic review. *arXiv preprint arXiv:2204.14081*, 2022.
- Kamyar Ghasemipour, Shixiang Shane Gu, and Ofir Nachum. Why so pessimistic? estimating uncertainties for offline rl through ensembles, and why their independence matters. *Advances in Neural Information Processing Systems*, 35:18267–18281, 2022.
- Shangding Gu, Long Yang, Yali Du, Guang Chen, Florian Walter, Jun Wang, Yaodong Yang, and Alois Knoll. A review of safe reinforcement learning: Methods, theory and applications. *arXiv preprint arXiv:2205.10330*, 2022.

- Abhishek Gupta, Russell Mendonca, YuXuan Liu, Pieter Abbeel, and Sergey Levine. Meta-reinforcement learning of structured exploration strategies. *Advances in neural information processing systems*, 31, 2018.
- Samarth Gupta, Shreyas Chaudhari, Subhojyoti Mukherjee, Gauri Joshi, and Osman Yağın. A unified approach to translate classical bandit algorithms to the structured bandit setting. *IEEE Journal on Selected Areas in Information Theory*, 1(3):840–853, 2020.
- Joey Hong, Branislav Kveton, Manzil Zaheer, Yinlam Chow, Amr Ahmed, and Craig Boutilier. Latent bandits revisited. *Advances in Neural Information Processing Systems*, 33:13423–13433, 2020.
- Joey Hong, Branislav Kveton, Sumeet Katariya, Manzil Zaheer, and Mohammad Ghavamzadeh. Deep hierarchy in bandits. In *International Conference on Machine Learning*, pages 8833–8851. PMLR, 2022a.
- Joey Hong, Branislav Kveton, Manzil Zaheer, and Mohammad Ghavamzadeh. Hierarchical bayesian bandits. In *International Conference on Artificial Intelligence and Statistics*, pages 7724–7741. PMLR, 2022b.
- Michael Janner, Qiyang Li, and Sergey Levine. Offline reinforcement learning as one big sequence modeling problem. *Advances in neural information processing systems*, 34:1273–1286, 2021.
- Yiding Jiang, Evan Liu, Benjamin Eysenbach, J Zico Kolter, and Chelsea Finn. Learning options via compression. *Advances in Neural Information Processing Systems*, 35:21184–21199, 2022.
- Richard Arnold Johnson, Dean W Wichern, et al. Applied multivariate statistical analysis. 2002.
- Kwang-Sung Jun, Rebecca Willett, Stephen Wright, and Robert Nowak. Bilinear bandits with low-rank structure. In *International Conference on Machine Learning*, pages 3163–3172. PMLR, 2019.
- Daniel Justus, John Brennan, Stephen Bonner, and Andrew Stephen McGough. Predicting the computational cost of deep learning models. In *2018 IEEE international conference on big data (Big Data)*, pages 3873–3882. IEEE, 2018.
- Yue Kang, Cho-Jui Hsieh, and Thomas Chun Man Lee. Efficient frameworks for generalized low-rank matrix bandit problems. *Advances in Neural Information Processing Systems*, 35:19971–19983, 2022.
- Aviral Kumar, Justin Fu, Matthew Soh, George Tucker, and Sergey Levine. Stabilizing off-policy q-learning via bootstrapping error reduction. *Advances in Neural Information Processing Systems*, 32, 2019.
- Aviral Kumar, Aurick Zhou, George Tucker, and Sergey Levine. Conservative q-learning for offline reinforcement learning. *Advances in Neural Information Processing Systems*, 33:1179–1191, 2020.
- Branislav Kveton, Csaba Szepesvári, Anup Rao, Zheng Wen, Yasin Abbasi-Yadkori, and S Muthukrishnan. Stochastic low-rank bandits. *arXiv preprint arXiv:1712.04644*, 2017.
- Jeongyeol Kwon, Yonathan Efroni, Constantine Caramanis, and Shie Mannor. Tractable optimality in episodic latent mabs. *Advances in Neural Information Processing Systems*, 35:23634–23645, 2022.
- Nicholas C Landolfi, Garrett Thomas, and Tengyu Ma. A model-based approach for sample-efficient multi-task reinforcement learning. *arXiv preprint arXiv:1907.04964*, 2019.
- Michael Laskin, Luyu Wang, Junhyuk Oh, Emilio Parisotto, Stephen Spencer, Richie Steigerwald, DJ Strouse, Steven Hansen, Angelos Filos, Ethan Brooks, et al. In-context reinforcement learning with algorithm distillation. *arXiv preprint arXiv:2210.14215*, 2022.
- Tor Lattimore and Csaba Szepesvári. An information-theoretic approach to minimax regret in partial monitoring. In *Conference on Learning Theory*, pages 2111–2139. PMLR, 2019.
- Tor Lattimore and Csaba Szepesvári. *Bandit algorithms*. Cambridge University Press, 2020.

- Mikko Lauri, David Hsu, and Joni Pajarinen. Partially observable markov decision processes in robotics: A survey. *IEEE Transactions on Robotics*, 39(1):21–40, 2022.
- Jonathan N Lee, Annie Xie, Aldo Pacchiano, Yash Chandak, Chelsea Finn, Ofir Nachum, and Emma Brunskill. Supervised pretraining can learn in-context reinforcement learning. *arXiv preprint arXiv:2306.14892*, 2023.
- Kuang-Huei Lee, Ofir Nachum, Mengjiao Sherry Yang, Lisa Lee, Daniel Freeman, Sergio Guadarrama, Ian Fischer, Winnie Xu, Eric Jang, Henryk Michalewski, et al. Multi-game decision transformers. *Advances in Neural Information Processing Systems*, 35:27921–27936, 2022.
- Langqing Li, Rui Yang, and Dijun Luo. Focal: Efficient fully-offline meta-reinforcement learning via distance metric learning and behavior regularization. *arXiv preprint arXiv:2010.01112*, 2020.
- Lihong Li, Wei Chu, John Langford, and Robert E Schapire. A contextual-bandit approach to personalized news article recommendation. In *Proceedings of the 19th international conference on World wide web*, pages 661–670, 2010.
- Lihong Li, Yu Lu, and Dengyong Zhou. Provably optimal algorithms for generalized linear contextual bandits. In *International Conference on Machine Learning*, pages 2071–2080. PMLR, 2017.
- Yingcong Li, Muhammed Emrullah Ildiz, Dimitris Papailiopoulos, and Samet Oymak. Transformers as algorithms: Generalization and stability in in-context learning. In *International Conference on Machine Learning*, pages 19565–19594. PMLR, 2023.
- Licong Lin, Yu Bai, and Song Mei. Transformers as decision makers: Provable in-context reinforcement learning via supervised pretraining. *arXiv preprint arXiv:2310.08566*, 2023.
- Evan Z Liu, Aditi Raghunathan, Percy Liang, and Chelsea Finn. Decoupling exploration and exploitation for meta-reinforcement learning without sacrifices. In *International conference on machine learning*, pages 6925–6935. PMLR, 2021.
- Xiaoqian Liu, Jianbin Jiao, and Junge Zhang. Self-supervised pretraining for decision foundation model: Formulation, pipeline and challenges. *arXiv preprint arXiv:2401.00031*, 2023a.
- Xin Liu, Daniel McDuff, Geza Kovacs, Isaac Galatzer-Levy, Jacob Sunshine, Jiening Zhan, Ming-Zher Poh, Shun Liao, Paolo Di Achille, and Shwetak Patel. Large language models are few-shot health learners. *arXiv preprint arXiv:2305.15525*, 2023b.
- Yao Liu, Adith Swaminathan, Alekh Agarwal, and Emma Brunskill. Off-policy policy gradient with state distribution correction. *arXiv preprint arXiv:1904.08473*, 2019.
- Yao Liu, Adith Swaminathan, Alekh Agarwal, and Emma Brunskill. Provably good batch off-policy reinforcement learning without great exploration. *Advances in neural information processing systems*, 33:1264–1274, 2020.
- Zhihan Liu, Hao Hu, Shenao Zhang, Hongyi Guo, Shuqi Ke, Boyi Liu, and Zhaoran Wang. Reason for future, act for now: A principled framework for autonomous llm agents with provable sample efficiency. *arXiv preprint arXiv:2309.17382*, 2023c.
- Chris Lu, Yannick Schroecker, Albert Gu, Emilio Parisotto, Jakob Foerster, Satinder Singh, and Feryal Behbahani. Structured state space models for in-context reinforcement learning. *arXiv preprint arXiv:2303.03982*, 2023.
- Yangyi Lu, Amirhossein Meisami, and Ambuj Tewari. Low-rank generalized linear bandit problems. In *International Conference on Artificial Intelligence and Statistics*, pages 460–468. PMLR, 2021.
- Yi Ma, Chenjun Xiao, Hebin Liang, and Jianye Hao. Rethinking decision transformer via hierarchical reinforcement learning. *arXiv preprint arXiv:2311.00267*, 2023.
- Andrea Madotto, Zhaojiang Lin, Genta Indra Winata, and Pascale Fung. Few-shot bot: Prompt-based learning for dialogue systems. *arXiv preprint arXiv:2110.08118*, 2021.
- Stefan Magureanu, Richard Combes, and Alexandre Proutiere. Lipschitz bandits: Regret lower bound and optimal algorithms. In *Conference on Learning Theory*, pages 975–999. PMLR, 2014.

- Odalric-Ambrym Maillard and Shie Mannor. Latent bandits. In *International Conference on Machine Learning*, pages 136–144. PMLR, 2014.
- Sewon Min, Xinxu Lyu, Ari Holtzman, Mikel Artetxe, Mike Lewis, Hannaneh Hajishirzi, and Luke Zettlemoyer. Rethinking the role of demonstrations: What makes in-context learning work? *arXiv preprint arXiv:2202.12837*, 2022.
- Suvir Mirchandani, Fei Xia, Pete Florence, Brian Ichter, Danny Driess, Montserrat Gonzalez Arenas, Kanishka Rao, Dorsa Sadigh, and Andy Zeng. Large language models as general pattern machines. *arXiv preprint arXiv:2307.04721*, 2023.
- Nikhil Mishra, Mostafa Rohaninejad, Xi Chen, and Pieter Abbeel. A simple neural attentive meta-learner. *arXiv preprint arXiv:1707.03141*, 2017.
- Eric Mitchell, Rafael Rafailov, Xue Bin Peng, Sergey Levine, and Chelsea Finn. Offline meta-reinforcement learning with advantage weighting. In *International Conference on Machine Learning*, pages 7780–7791. PMLR, 2021.
- Volodymyr Mnih, Koray Kavukcuoglu, David Silver, Alex Graves, Ioannis Antonoglou, Daan Wierstra, and Martin Riedmiller. Playing atari with deep reinforcement learning. *arXiv preprint arXiv:1312.5602*, 2013.
- Subhojyoti Mukherjee, Qiaomin Xie, Josiah P Hanna, and Robert Nowak. Multi-task representation learning for pure exploration in bilinear bandits. *arXiv preprint arXiv:2311.00327*, 2023.
- Samuel Müller, Noah Hollmann, Sebastian Pineda Arango, Josif Grabocka, and Frank Hutter. Transformers can do bayesian inference. *arXiv preprint arXiv:2112.10510*, 2021.
- Susan A Murphy. Optimal dynamic treatment regimes. *Journal of the Royal Statistical Society Series B: Statistical Methodology*, 65(2):331–355, 2003.
- Anusha Nagabandi, Ignasi Clavera, Simin Liu, Ronald S Fearing, Pieter Abbeel, Sergey Levine, and Chelsea Finn. Learning to adapt in dynamic, real-world environments through meta-reinforcement learning. *arXiv preprint arXiv:1803.11347*, 2018.
- Behnam Neyshabur, Ryota Tomioka, Ruslan Salakhutdinov, and Nathan Srebro. Geometry of optimization and implicit regularization in deep learning. *arXiv preprint arXiv:1705.03071*, 2017.
- Soumyabrata Pal, Arun Sai Suggala, Karthikeyan Shanmugam, and Prateek Jain. Optimal algorithms for latent bandits with cluster structure. In *International Conference on Artificial Intelligence and Statistics*, pages 7540–7577. PMLR, 2023.
- Theodore J Perkins and Doina Precup. Using options for knowledge transfer in reinforcement learning title2, 1999.
- Vitchyr H Pong, Ashvin V Nair, Laura M Smith, Catherine Huang, and Sergey Levine. Offline meta-reinforcement learning with online self-supervision. In *International Conference on Machine Learning*, pages 17811–17829. PMLR, 2022.
- Friedrich Pukelsheim. *Optimal design of experiments*. SIAM, 2006.
- Kate Rakelly, Aurick Zhou, Chelsea Finn, Sergey Levine, and Deirdre Quillen. Efficient off-policy meta-reinforcement learning via probabilistic context variables. In *International conference on machine learning*, pages 5331–5340. PMLR, 2019.
- Scott Reed, Konrad Zolna, Emilio Parisotto, Sergio Gomez Colmenarejo, Alexander Novikov, Gabriel Barth-Maron, Mai Gimenez, Yury Sulsky, Jackie Kay, Jost Tobias Springenberg, et al. A generalist agent. *arXiv preprint arXiv:2205.06175*, 2022.
- Carlos Riquelme, George Tucker, and Jasper Snoek. Deep bayesian bandits showdown: An empirical comparison of bayesian deep networks for thompson sampling. *arXiv preprint arXiv:1802.09127*, 2018.

- Adam Roberts, Colin Raffel, Katherine Lee, Michael Matena, Noam Shazeer, Peter J Liu, Sharan Narang, Wei Li, and Yanqi Zhou. Exploring the limits of transfer learning with a unified text-to-text transformer. 2019.
- Jonas Rothfuss, Dennis Lee, Ignasi Clavera, Tamim Asfour, and Pieter Abbeel. Prompt: Proximal meta-policy search. *arXiv preprint arXiv:1810.06784*, 2018.
- Daniel J Russo, Benjamin Van Roy, Abbas Kazerooni, Ian Osband, Zheng Wen, et al. A tutorial on thompson sampling. *Foundations and Trends® in Machine Learning*, 11(1):1–96, 2018.
- Tom Schaul and Jürgen Schmidhuber. Metalearning. *Scholarpedia*, 5(6):4650, 2010.
- Sina Semnani, Violet Yao, Heidi Zhang, and Monica Lam. Wikichat: Stopping the hallucination of large language model chatbots by few-shot grounding on wikipedia. In *Findings of the Association for Computational Linguistics: EMNLP 2023*, pages 2387–2413, 2023.
- Nur Muhammad Shafiullah, Zichen Cui, Ariuntuya Arty Altanzaya, and Lerrel Pinto. Behavior transformers: Cloning  $k$  modes with one stone. *Advances in neural information processing systems*, 35:22955–22968, 2022.
- Noah Y Siegel, Jost Tobias Springenberg, Felix Berkenkamp, Abbas Abdolmaleki, Michael Neunert, Thomas Lampe, Roland Hafner, Nicolas Heess, and Martin Riedmiller. Keep doing what worked: Behavioral modelling priors for offline reinforcement learning. *arXiv preprint arXiv:2002.08396*, 2020.
- Viacheslav Sinii, Alexander Nikulin, Vladislav Kurenkov, Ilya Zisman, and Sergey Kolesnikov. In-context reinforcement learning for variable action spaces. *arXiv preprint arXiv:2312.13327*, 2023.
- Daniel Soudry, Elad Hoffer, Mor Shpigel Nacson, Suriya Gunasekar, and Nathan Srebro. The implicit bias of gradient descent on separable data. *Journal of Machine Learning Research*, 19(70):1–57, 2018.
- Richard S Sutton and Andrew G Barto. *Reinforcement learning: An introduction*. MIT press, 2018.
- William R Thompson. On the likelihood that one unknown probability exceeds another in view of the evidence of two samples. *Biometrika*, 25(3-4):285–294, 1933.
- Sabina Tomkins, Peng Liao, Predrag Klasnja, Serena Yeung, and Susan Murphy. Rapidly personalizing mobile health treatment policies with limited data. *arXiv preprint arXiv:2002.09971*, 2020.
- Michal Valko, Nathaniel Korda, Rémi Munos, Ilias Flaounas, and Nelo Cristianini. Finite-time analysis of kernelised contextual bandits. *arXiv preprint arXiv:1309.6869*, 2013.
- Ashish Vaswani, Noam Shazeer, Niki Parmar, Jakob Uszkoreit, Llion Jones, Aidan N Gomez, Lukasz Kaiser, and Illia Polosukhin. Attention is all you need. *Advances in neural information processing systems*, 30, 2017.
- Jane X Wang, Zeb Kurth-Nelson, Dhruva Tirumala, Hubert Soyer, Joel Z Leibo, Remi Munos, Charles Blundell, Dharshan Kumaran, and Matt Botvinick. Learning to reinforcement learn. *arXiv preprint arXiv:1611.05763*, 2016.
- Yifan Wu, George Tucker, and Ofir Nachum. Behavior regularized offline reinforcement learning. *arXiv preprint arXiv:1911.11361*, 2019.
- Sang Michael Xie, Aditi Raghunathan, Percy Liang, and Tengyu Ma. An explanation of in-context learning as implicit bayesian inference. *arXiv preprint arXiv:2111.02080*, 2021.
- Adam X Yang, Maxime Robeyns, Xi Wang, and Laurence Aitchison. Bayesian low-rank adaptation for large language models. *arXiv preprint arXiv:2308.13111*, 2023.
- Jiaqi Yang, Wei Hu, Jason D Lee, and Simon S Du. Impact of representation learning in linear bandits. *arXiv preprint arXiv:2010.06531*, 2020.

- Jiaqi Yang, Qi Lei, Jason D Lee, and Simon S Du. Nearly minimax algorithms for linear bandits with shared representation. *arXiv preprint arXiv:2203.15664*, 2022a.
- Lin Yang and Mengdi Wang. Reinforcement learning in feature space: Matrix bandit, kernels, and regret bound. In *International Conference on Machine Learning*, pages 10746–10756. PMLR, 2020.
- Mengjiao Yang, Dale Schuurmans, Pieter Abbeel, and Ofir Nachum. Dichotomy of control: Separating what you can control from what you cannot. *arXiv preprint arXiv:2210.13435*, 2022b.
- Tianhe Yu, Aviral Kumar, Rafael Rafailov, Aravind Rajeswaran, Sergey Levine, and Chelsea Finn. Combo: Conservative offline model-based policy optimization. *Advances in neural information processing systems*, 34:28954–28967, 2021.
- Vinicius Zambaldi, David Raposo, Adam Santoro, Victor Bapst, Yujia Li, Igor Babuschkin, Karl Tuyls, David Reichert, Timothy Lillicrap, Edward Lockhart, et al. Relational deep reinforcement learning. *arXiv preprint arXiv:1806.01830*, 2018.
- Andrew Zhao, Daniel Huang, Quentin Xu, Matthieu Lin, Yong-Jin Liu, and Gao Huang. Expel: Llm agents are experiential learners. *arXiv preprint arXiv:2308.10144*, 2023.
- Dongruo Zhou, Lihong Li, and Quanquan Gu. Neural contextual bandits with ucb-based exploration. In *International Conference on Machine Learning*, pages 11492–11502. PMLR, 2020.
- Qiuyu Zhu and Vincent Tan. Thompson sampling algorithms for mean-variance bandits. In *International Conference on Machine Learning*, pages 11599–11608. PMLR, 2020.
- Luisa Zintgraf, Kyriacos Shiarlis, Maximilian Igl, Sebastian Schulze, Yarin Gal, Katja Hofmann, and Shimon Whiteson. Varibad: A very good method for bayes-adaptive deep rl via meta-learning. *arXiv preprint arXiv:1910.08348*, 2019.



## A Appendix

### A.1 Related Works

In this section, we briefly discuss related works.

In-context decision making [Laskin et al., 2022, Lee et al., 2023] has emerged as an attractive alternative in Reinforcement Learning (RL) compared to updating the model parameters after collection of new data [Mnih et al., 2013, François-Lavet et al., 2018]. In RL the contextual data takes the form of state-action-reward tuples representing a dataset of interactions with an unknown environment (task). In this paper, we will refer to this as the in-context data. Recall that in many real-world settings, the underlying task can be structured with correlated features, and the reward can be highly non-linear. So specialized bandit algorithms fail to learn in these tasks. To circumvent this issue, a learner can first collect in-context data consisting of just action indices  $I_t$  and rewards  $r_t$ . Then it can leverage the representation learning capability of deep neural networks to learn a pattern across the in-context data and subsequently derive a near-optimal policy [Lee et al., 2023, Mirchandani et al., 2023]. We refer to this learning framework as an in-context decision-making setting.

The in-context decision-making setting of Sinii et al. [2023] also allows changing the action space by learning an embedding over the action space yet also requires the optimal action during training. In contrast we do not require the optimal action as well as show that we can generalize to new actions without learning an embedding over them. Similarly, Lin et al. [2023] study the in-context decision-making setting of Laskin et al. [2022], Lee et al. [2023], but they also require a greedy approximation of the optimal action. The Ma et al. [2023] also studies a similar setting for hierarchical RL where they stitch together sub-optimal trajectories and predict the next action during test time. Similarly, Liu et al. [2023c] studies the in-context decision-making setting to predict action instead of learning a reward correlation from a short horizon setting. In contrast we do not require a greedy approximation of the optimal action, deal with short horizon setting and changing action sets during training and testing, and predict the estimated means of the actions instead of predicting the optimal action. A survey of the in-context decision-making approaches can be found in Liu et al. [2023a].

In the in-context decision-making setting, the learning model is first trained on supervised input-output examples with the in-context data during training. Then during test time, the model is asked to complete a new input (related to the context provided) without any update to the model parameters [Xie et al., 2021, Min et al., 2022]. Motivated by this, Lee et al. [2023] recently proposed the Decision Pretrained Transformers (DPT) that exhibit the following properties: (1) During supervised pretraining of DPT, predicting optimal actions alone gives rise to near-optimal decision-making algorithms for unforeseen task during test time. Note that DPT does not update model parameters during test time and, therefore, conducts in-context learning on the unforeseen task. (2) DPT improves over the in-context data used to pretrain it by exploiting latent structure. However, DPT either requires the optimal action during training or if it needs to approximate the optimal action. For approximating the optimal action, it requires a large amount of data from the underlying task.

At the same time, learning the underlying data pattern from a few examples during training is becoming more relevant in many domains like chatbot interaction [Madotto et al., 2021, Semnani et al., 2023], recommendation systems, healthcare [Ge et al., 2022, Liu et al., 2023b], etc. This is referred to as few-shot learning. However, most current RL decision-making systems (including in-context learners like DPT) require an enormous amount of data to learn a good policy.

The in-context learning framework is related to the meta-learning framework [Bengio et al., 1990, Schaul and Schmidhuber, 2010]. Broadly, these techniques aim to learn the underlying latent shared structure within the training distribution of tasks, facilitating faster learning of novel tasks during test time. In the context of decision-making and reinforcement learning (RL), there exists a frequent choice regarding the specific 'structure' to be learned, be it the task dynamics [Fu et al., 2016, Nagabandi et al., 2018, Landolfi et al., 2019], a task context identifier [Rakelly et al., 2019, Zintgraf et al., 2019, Liu et al., 2021], or temporally extended skills and options [Perkins and Precup, 1999, Gupta et al., 2018, Jiang et al., 2022].

However, as we noted in the Section 1, one can do a greedy approximation of the optimal action from the historical data using a weak demonstrator and a neural network policy [Finn et al., 2017, Rothfuss et al., 2018]. Moreover, the in-context framework generally is more agnostic where it learns the policy of the demonstrator [Duan et al., 2016, Wang et al., 2016, Mishra et al., 2017]. Note that

both **DPT-greedy** and **PreDeToR** are different than algorithmic distillation [Laskin et al., 2022, Lu et al., 2023] as they do not distill an existing RL algorithm. moreover, in contrast to **DPT-greedy** which is trained to predict the optimal action, the **PreDeToR** is trained to predict the reward for each of the actions. This enables the **PreDeToR** (similar to **DPT-greedy**) to show to potentially emergent online and offline strategies at test time that automatically align with the task structure, resembling posterior sampling.

As we discussed in the Section 1, in decision-making, RL, and imitation learning the transformer models are trained using autoregressive action prediction [Yang et al., 2023]. Similar methods have also been used in Large language models [Vaswani et al., 2017, Roberts et al., 2019]. One of the more notable examples is the Decision Transformers (abbreviated as DT) which utilizes a transformer to autoregressively model sequences of actions from offline experience data, conditioned on the achieved return [Chen et al., 2021, Janner et al., 2021]. This approach has also been shown to be effective for multi-task settings [Lee et al., 2022], and multi-task imitation learning with transformers [Reed et al., 2022, Brohan et al., 2022, Shafiqullah et al., 2022]. However, the DT methods are not known to improve upon their in-context data, which is the main thrust of this paper [Brandfonbrener et al., 2022, Yang et al., 2022b].

Our work is also closely related to the offline RL setting. In offline RL, the algorithms can formulate a policy from existing data sets of state, action, reward, and next-state interactions. Recently, the idea of pessimism has also been introduced in an offline setting to address the challenge of distribution shift [Kumar et al., 2020, Yu et al., 2021, Liu et al., 2020, Ghasemipour et al., 2022]. Another approach to solve this issue is policy regularization [Fujimoto et al., 2019, Kumar et al., 2019, Wu et al., 2019, Siegel et al., 2020, Liu et al., 2019], or reuse data for related task [Li et al., 2020, Mitchell et al., 2021], or additional collection of data along with offline data [Pong et al., 2022]. However, all of these approaches still have to take into account the issue of distributional shifts. In contrast **PreDeToR** and **DPT-greedy** leverages the decision transformers to avoid these issues. Both of these methods can also be linked to posterior sampling. Such connections between sequence modeling with transformers and posterior sampling have also been made in Chen et al. [2021], Müller et al. [2021], Lee et al. [2023], Yang et al. [2023].

## A.2 Experimental Setting Information

**Linear Bandit:** We consider the setting when  $f(\mathbf{x}, \theta_*) = \mathbf{x}^\top \theta_*$ . Here  $\mathbf{x} \in \mathbb{R}^d$  is the action feature and  $\theta_* \in \mathbb{R}^d$  is the hidden parameter. For every experiment, we first generate tasks from  $\mathcal{T}_{\text{pre}}$ . Then we sample a fixed set of actions from  $\mathcal{N}(\mathbf{0}, \mathbf{I}_d/d)$  in  $\mathbb{R}^d$  and this constitutes the features. Then for each task  $m \in [M]$  we sample  $\theta_{m,*} \sim \mathcal{N}(\mathbf{0}, \mathbf{I}_d/d)$  to produce the means  $\mu(m, a) = \langle \theta_{m,*}, \mathbf{x}(m, a) \rangle$  for  $a \in \mathcal{A}$  and  $m \in [M]$ . Finally, note that we do not shuffle the data as the order matters. Also in this setting  $\mathbf{x}(m, a)$  for each  $a \in \mathcal{A}$  is fixed for all tasks  $m$ .

**Non-Linear Bandit:** We now consider the setting when  $f(\mathbf{x}, \theta_*) = 1/(1 + 0.5 \cdot \exp(2 \cdot \exp(-\mathbf{x}^\top \theta_*)))$ . Again, here  $\mathbf{x} \in \mathbb{R}^d$  is the action feature, and  $\theta_* \in \mathbb{R}^d$  is the hidden parameter. Note that this is different than the generalized linear bandit setting [Filippi et al., 2010, Li et al., 2017]. Again for every experiment, we first generate tasks from  $\mathcal{T}_{\text{pre}}$ . Then we sample a fixed set of actions from  $\mathcal{N}(\mathbf{0}, \mathbf{I}_d/d)$  in  $\mathbb{R}^d$  and this constitutes the features. Then for each task  $m \in [M]$  we sample  $\theta_{m,*} \sim \mathcal{N}(\mathbf{0}, \mathbf{I}_d/d)$  to produce the means  $\mu(m, a) = 1/(1 + 0.5 \cdot \exp(2 \cdot \exp(-\mathbf{x}(m, a)^\top \theta_{m,*})))$  for  $a \in \mathcal{A}$  and  $m \in [M]$ . Again note that in this setting  $\mathbf{x}(m, a)$  for each  $a \in \mathcal{A}$  is fixed for all tasks  $m$ .

We use NVIDIA GeForce RTX 3090 GPU with 24GB RAM to load the GPT 2 Large Language Model. This requires less than 2GB RAM without data, and with large context may require as much as 20GB RAM.

## A.3 Empirical Study: Bilinear Bandits

In this section, we discuss the performance of **PreDeToR** against the other baselines in the bilinear setting. Again note that the number of tasks  $M_{\text{pre}} \gg A \geq n$ . Through this experiment, we want to evaluate the performance of **PreDeToR** to exploit the underlying latent structure and reward correlation when the horizon is small, the number of tasks is large, and understand its performance in the bilinear bandit setting [Jun et al., 2019, Lu et al., 2021, Kang et al., 2022, Mukherjee et al.,

2023]. Note that this setting also goes beyond the linear feedback model [Abbasi-Yadkori et al., 2011, Lattimore and Szepesvári, 2020] and is related to matrix bandits [Yang and Wang, 2020].

**Bilinear bandit setting:** In the bilinear bandits the learner is provided with two sets of action sets,  $\mathcal{X} \subseteq \mathbb{R}^{d_1}$  and  $\mathcal{Z} \subseteq \mathbb{R}^{d_2}$  which are referred to as the left and right action sets. At every round  $t$  the learner chooses a pair of actions  $\mathbf{x}_t \in \mathcal{X}$  and  $\mathbf{z}_t \in \mathcal{Z}$  and observes a reward

$$r_t = \mathbf{x}_t^\top \Theta_* \mathbf{z}_t + \eta_t$$

where  $\Theta_* \in \mathbb{R}^{d_1 \times d_2}$  is the unknown hidden matrix which is also low-rank. The  $\eta_t$  is a  $\sigma^2$  sub-Gaussian noise. In the multi-task bilinear bandit setting we now have a set of  $M$  tasks where the reward for the  $m$ -th task at round  $t$  is given by

$$r_{m,t} = \mathbf{x}_{m,t}^\top \Theta_{m,*} \mathbf{z}_{m,t} + \eta_{m,t}.$$

Here  $\Theta_{m,*} \in \mathbb{R}^{d_1 \times d_2}$  is the unknown hidden matrix for each task  $m$ , which is also low-rank. The  $\eta_{m,t}$  is a  $\sigma^2$  sub-Gaussian noise. Let  $\kappa$  be the rank of each of these matrices  $\Theta_{m,*}$ .

A special case is the rank 1 structure where  $\Theta_{m,*} = \theta_{m,*} \theta_{m,*}^\top$  where  $\theta_{m,*} \in \mathbb{R}^{d \times d}$  and  $\theta_{m,*} \in \mathbb{R}^d$  for each task  $m$ . Let the left and right action sets be also same such that  $\mathbf{x}_{m,t} \in \mathcal{X} \subseteq \mathbb{R}^d$ . Observe then that the reward for the  $m$ -th task at round  $t$  is given by

$$r_{m,t} = \mathbf{x}_{m,t}^\top \theta_{m,*} \mathbf{x}_{m,t} + \eta_{m,t} = (\mathbf{x}_{m,t}^\top \theta_{m,*})^2 + \eta_{m,t}.$$

This special case is studied in Chaudhuri et al. [2017].

**Baselines:** We again implement the same baselines discussed in Section 4. The baselines are PreDeToR, PreDeToR- $\tau$ , DPT-greedy, and Thomp. However, we now implement the LowOFUL [Jun et al., 2019] which is optimal in the bilinear bandit setting.

**LowOFUL:** The LowOFUL algorithm first estimates the unknown parameter  $\Theta_{m,*}$  for each task  $m$  using E-optimal design [Pukelsheim, 2006, Fedorov, 2013, Jun et al., 2019] for  $n_1$  rounds. Let  $\hat{\Theta}_{m,n_1}$  be the estimate of  $\Theta_{m,*}$  at the end of  $n_1$  rounds. Let the SVD of  $\hat{\Theta}_{m,n_1}$  be given by  $\text{SVD}(\hat{\Theta}_{m,n_1}) = \hat{\mathbf{U}}_{m,n_1} \hat{\mathbf{S}}_{m,n_1} \hat{\mathbf{V}}_{m,n_1}^\top$ . Then LowOFUL rotates the actions as follows:

$$\mathcal{X}'_m = \left\{ \left[ \hat{\mathbf{U}}_{m,n_1} \hat{\mathbf{U}}_{m,n_1}^\perp \right]^\top \mathbf{x}_m : \mathbf{x}_m \in \mathcal{X} \right\} \text{ and } \mathcal{Z}'_m = \left\{ \left[ \hat{\mathbf{V}}_{m,n_1} \hat{\mathbf{V}}_{m,n_1}^\perp \right]^\top \mathbf{z}_m : \mathbf{z}_m \in \mathcal{Z} \right\}.$$

Then defines a vectorized action set for each task  $m$  so that the last  $(d_1 - \kappa) \cdot (d_2 - \kappa)$  components are from the complementary subspaces:

$$\tilde{\mathcal{A}}_m = \left\{ \left[ \text{vec}(\mathbf{x}_{m,1:\kappa} \mathbf{z}_{m,1:\kappa}^\top); \text{vec}(\mathbf{x}_{m,\kappa+1:d_1} \mathbf{z}_{m,1:\kappa}^\top); \text{vec}(\mathbf{x}_{m,1:\kappa} \mathbf{z}_{m,\kappa+1:d_2}^\top); \text{vec}(\mathbf{x}_{m,\kappa+1:d_1} \mathbf{z}_{m,\kappa+1:d_2}^\top) \right] \in \mathbb{R}^{d_1 d_2} : \mathbf{x}_m \in \mathcal{X}'_m, \mathbf{z}_m \in \mathcal{Z}'_m \right\}.$$

Finally for  $n_2 = n - n_1$  rounds, LowOFUL invokes the specialized OFUL algorithm [Abbasi-Yadkori et al., 2011] for the rotated action set  $\tilde{\mathcal{A}}_m$  with the low dimension  $k = (d_1 + d_2) \kappa - \kappa^2$ . Note that the LowOFUL runs the per-task low dimensional OFUL algorithm rather than learning the underlying structure across the tasks [Mukherjee et al., 2023].

**Outcomes:** We first discuss the main outcomes of our experimental results for increasing the horizon:

- (1) The PreDeToR ( $-\tau$ ) learns to exploit the underlying latent bilinear structure and reward correlation between the different tasks even when  $A \geq n$  but  $M_{\text{pre}} \gg A$ .
- (2) The PreDeToR ( $-\tau$ ) has lower regret than its weak demonstrator Thomp which does not know the underlying bilinear structure.
- (3) The PreDeToR ( $-\tau$ ) has lower regret compared to DPT-greedy and AD. Also, observe that PreDeToR matches the performance of LowOFUL.

**Experimental Result:** We observe these outcomes in Figure 3. In Figure 3(a) we experiment with rank 1 hidden parameter  $\Theta_{m,*}$  and set horizon  $n = 20$ ,  $M_{\text{pre}} = 200000$ ,  $M_{\text{test}} = 200$ ,  $A = 30$ , and  $d = 5$ . In Figure 3(b) we experiment with rank 2 hidden parameter  $\Theta_{m,*}$  and set horizon  $n = 20$ ,  $M_{\text{pre}} = 250000$ ,  $M_{\text{test}} = 200$ ,  $A = 25$ , and  $d = 5$ . Again, the demonstrator  $\pi^w$  is the Thomp algorithm. We observe that PreDeToR has lower cumulative regret than DPT-greedy, AD and Thomp.

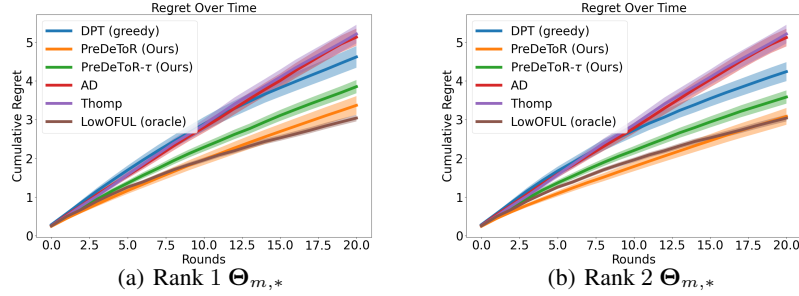


Figure 3: Experiment with bilinear bandits. The y-axis shows the cumulative regret.

Note that for any task  $m$  for the horizon 20 the **Thomp** will be able to sample all the actions at most once. Note that for this small horizon setting the **DPT-greedy** does not have a good estimation of  $\hat{a}_{m,*}$  which results in a poor prediction of optimal action  $\hat{a}_{m,t,*}$ . In contrast **PreDeToR** learns the correlation of rewards across tasks and can perform well. Observe from Figure 3(a), and 3(b) that **PreDeToR** has lower regret than **Thomp** and matches **LowOFUL**. Also, in this low-data regime it is not enough for **LowOFUL** to learn the underlying  $\Theta_{m,*}$  with high precision. Hence, **PreDeToR** also has slightly lower regret than **LowOFUL**. The training of **AD** ensures that it does not outperform the demonstrator **Thomp**. Most importantly it shows that **PreDeToR** can exploit the underlying latent structure and reward correlation better than **DPT-greedy**, and **AD**.

#### A.4 Empirical Study: Latent Bandits

In this section, we discuss the performance of **PreDeToR** ( $-\tau$ ) against the other baselines in the latent bandit setting and create a generalized bilinear bandit setting. Note that the number of tasks  $M_{\text{pre}} \gg A \geq n$ . Using this experiment, we want to evaluate the ability of **PreDeToR** ( $-\tau$ ) to exploit the underlying reward correlation when the horizon is small, the number of tasks is large, and understand its performance in the latent bandit setting [Hong et al., 2020, Maillard and Mannor, 2014, Pal et al., 2023, Kveton et al., 2017]. We create a latent bandit setting which generalizes the bilinear bandit setting [Jun et al., 2019, Lu et al., 2021, Kang et al., 2022, Mukherjee et al., 2023]. Again note that this setting also goes beyond the linear feedback model [Abbasi-Yadkori et al., 2011, Lattimore and Szepesvári, 2020] and is related to matrix bandits [Yang and Wang, 2020].

**Latent bandit setting:** In this special multi-task latent bandits the learner is again provided with two sets of action sets,  $\mathcal{X} \subseteq \mathbb{R}^{d_1}$  and  $\mathcal{Z} \subseteq \mathbb{R}^{d_2}$  which are referred to as the left and right action sets. The reward for the  $m$ -th task at round  $t$  is given by

$$r_{m,t} = \mathbf{x}_{m,t}^\top \underbrace{(\Theta_{m,*} + \mathbf{U}\mathbf{V}^\top)}_{\mathbf{Z}_{m,*}} \mathbf{z}_{m,t} + \eta_{m,t}.$$

Here  $\Theta_{m,*} \in \mathbb{R}^{d_1 \times d_2}$  is the unknown hidden matrix for each task  $m$ , which is also low-rank. Additionally, all the tasks share a *common latent parameter matrix*  $\mathbf{U}\mathbf{V}^\top \in \mathbb{R}^{d_1 \times d_2}$  which is also low rank. Hence the learner needs to learn the latent parameter across the tasks hence the name latent bandits. Finally, the  $\eta_{m,t}$  is a  $\sigma^2$  sub-Gaussian noise. Let  $\kappa$  be the rank of each of these matrices  $\Theta_{m,*}$  and  $\mathbf{U}\mathbf{V}^\top$ . Again special case is the rank 1 structure where the reward for the  $m$ -th task at round  $t$  is given by

$$r_{m,t} = \mathbf{x}_{m,t}^\top \underbrace{(\boldsymbol{\theta}_{m,*} \boldsymbol{\theta}_{m,*}^\top + \mathbf{u}\mathbf{v}^\top)}_{\mathbf{Z}_{m,*}} \mathbf{x}_{m,t} + \eta_{m,t}.$$

where  $\boldsymbol{\theta}_{m,*} \in \mathbb{R}^d$  for each task  $m$  and  $\mathbf{u}, \mathbf{v} \in \mathbb{R}^d$ . Note that the left and right action sets are the same such that  $\mathbf{x}_{m,t} \in \mathcal{X} \subseteq \mathbb{R}^d$ .

**Baselines:** We again implement the same baselines discussed in Section 4. The baselines are **PreDeToR**, **PreDeToR- $\tau$** , **DPT-greedy**, **AD**, **Thomp**, and **LowOFUL**. However, we now implement a special **LowOFUL** (stated in Appendix A.3) which has knowledge of the shared latent parameters  $\mathbf{U}$ , and  $\mathbf{V}$ . We call this the **LowOFUL (oracle)** algorithm. Therefore **LowOFUL (oracle)** has knowledge of the problem parameters in the latent bandit setting and hence the name.

**Outcomes:** We first discuss the main outcomes of our experimental results for increasing the horizon:

- (1) The **PreDeToR** ( $-\tau$ ) learns to exploit the underlying latent bilinear structure and reward correlation between the different tasks even when  $A \geq n$  but  $M_{\text{pre}} \gg A$ .
- (2) The **PreDeToR** ( $-\tau$ ) has lower regret than its weak demonstrator **Thomp** which does not know the underlying latent structure. The **PreDeToR** ( $-\tau$ ) has lower regret compared to **DPT-greedy**.
- (3) The **PreDeToR** ( $-\tau$ ) has regret that is closer to **LowOFUL** (oracle).

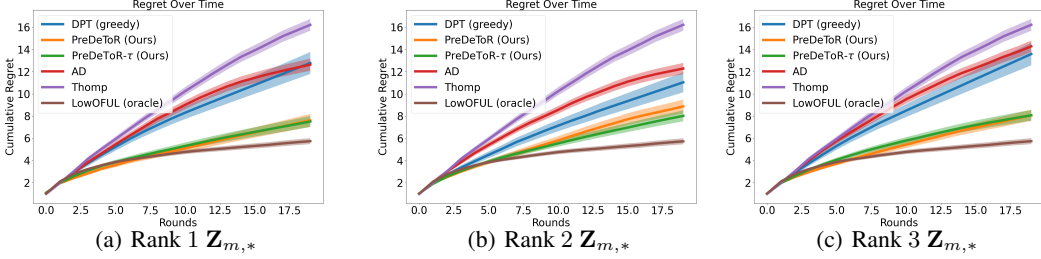


Figure 4: Experiment with latent bandits. The y-axis shows the cumulative regret.

**Experimental Result:** We observe these outcomes in Figure 4. In Figure 4(a) we experiment with rank 1 hidden parameter  $\theta_{m,*} \theta_{m,*}^\top$  and latent parameters  $\mathbf{u}\mathbf{v}^\top$  shared across the tasks and set horizon  $n = 20$ ,  $M_{\text{pre}} = 200000$ ,  $M_{\text{test}} = 200$ ,  $A = 30$ , and  $d = 5$ . In Figure 4(b) we experiment with rank 2 hidden parameter  $\Theta_{m,*}$ , and latent parameters  $\mathbf{U}\mathbf{V}^\top$  and set horizon  $n = 20$ ,  $M_{\text{pre}} = 250000$ ,  $M_{\text{test}} = 200$ ,  $A = 25$ , and  $d = 5$ . In Figure 4(c) we experiment with rank 3 hidden parameter  $\Theta_{m,*}$ , and latent parameters  $\mathbf{U}\mathbf{V}^\top$  and set horizon  $n = 20$ ,  $M_{\text{pre}} = 300000$ ,  $M_{\text{test}} = 200$ ,  $A = 25$ , and  $d = 5$ . Again, the demonstrator  $\pi^w$  is the **Thomp** algorithm. We observe that **PreDeToR** ( $-\tau$ ) has lower cumulative regret than **DPT-greedy**, **AD** and **Thomp**. Note that for any task  $m$  for the horizon 20 the **Thomp** will be able to sample all the actions at most once. Note that for this small horizon setting the **DPT-greedy** does not have a good estimation of  $\hat{a}_{m,*}$  which results in a poor prediction of optimal action  $\hat{a}_{m,t,*}$ . In contrast **PreDeToR** ( $-\tau$ ) learns the correlation of rewards across tasks and is able to perform well. Observe from Figure 4(a), 4(b), and 4(c) that **PreDeToR** has lower regret than **Thomp** and has regret closer to **LowOFUL** (oracle) which has access to the problem-dependent parameters. Hence, **LowOFUL** (oracle) outperforms **PreDeToR** ( $-\tau$ ) in this setting. The training of **AD** ensures that it does not outperform the demonstrator **Thomp**. This shows that **PreDeToR** is able to exploit the underlying latent structure and reward correlation better than **DPT-greedy**, and **AD**.

## A.5 Understanding **PreDeToR**

In this section, we try to understand the behavior of **PreDeToR** and its ability to exploit the reward correlation across tasks under a *linear multivariate Gaussian model*. In this model, the hidden task parameter,  $\theta_*$ , is a random variable drawn from a multi-variate Gaussian distribution [Bishop, 2006] and the feedback follows a linear model. We study this setting since we can estimate the Linear Minimum Mean Square Estimator (LMMSE) in this setting [Carlin and Louis, 2008, Box and Tiao, 2011]. This yields a posterior prediction for the mean of each action over all tasks on average, by leveraging the linear structure when  $\theta_*$  is drawn from a multi-variate Gaussian distribution. So we can compare the performance of **PreDeToR** against such an LMMSE and evaluate whether it is exploiting the underlying linear structure and the reward correlation across tasks.

Consider the linear feedback setting consisting of  $A$  actions and the hidden task parameter  $\theta_* \sim \mathcal{N}(0, \sigma_\theta^2 \mathbf{I}_d)$ . The reward of the action  $\mathbf{x}_t$  at round  $t$  is given by  $r_t = \mathbf{x}_t^\top \theta_* + \eta_t$ , where  $\eta_t$  is  $\sigma^2$  sub-Gaussian. Let  $\pi^w$  collect  $n$  rounds of pretraining in-context data and observe  $\{I_t, r_t\}_{t=1}^n$ . Let  $N_n(a)$  denote the total number of times the action  $a$  is sampled for  $n$  rounds. Note that we drop the task index  $m$  in these notations as the random variable  $\theta_*$  corresponds to the task. Define the matrix  $\mathbf{H}_n \in \mathbb{R}^{n \times A}$  where the  $t$ -th row represents the action  $I_t$  for  $t \in [n]$ . The  $t$ -th row of  $\mathbf{H}_n$  is a one-hot vector with the  $I_t$ -th component being 1. We represent each action by one hot vector because we assume that this LMMSE does not have access to the feature vectors of the actions similar to the **PreDeToR** for fair comparison. Then define the reward vector  $\mathbf{Y}_n \in \mathbb{R}^n$  where the  $t$ -th component is the reward  $r_t$  observed for the action  $I_t$  for  $t \in [n]$  in the pretraining data. Define the diagonal matrix

$\mathbf{D}_A \in \mathbb{R}^{A \times A}$  estimated from pretraining data as follows

$$\mathbf{D}_A(i, i) = \begin{cases} \frac{\sigma^2}{N_n(a)}, & \text{if } N_n(a) > 0 \\ = 0, & \text{if } N_n(a) = 0 \end{cases} \quad (6)$$

where the reward noise being  $\sigma^2$  sub-Gaussian is known. Finally define the estimated reward covariance matrix  $\mathbf{S}_A \in \mathbb{R}^{A \times A}$  as  $\mathbf{S}_A(a, a') = \widehat{\mu}_n(a)\widehat{\mu}_n(a')$ , where  $\widehat{\mu}_n(a)$  is the empirical mean of action  $a$  estimated from the pretraining data. This matrix captures the reward correlation between the pairs of actions  $a, a' \in [A]$ . Then the posterior average mean estimator  $\widehat{\mu} \in \mathbb{R}^A$  over all tasks is given by the following lemma. The proof is given in Appendix B.1.

**Lemma 1.** *Let  $\mathbf{H}_n$  be the action matrix,  $\mathbf{Y}_n$  be the reward vector and  $\mathbf{S}_A$  be the estimated reward covariance matrix. Then the posterior prediction of the average mean reward vector  $\widehat{\mu}$  over all tasks is given by*

$$\widehat{\mu} = \sigma_{\theta}^2 \mathbf{S}_A \mathbf{H}_n^{\top} (\sigma_{\theta}^2 \mathbf{H}_n (\mathbf{S}_A + \mathbf{D}_A) \mathbf{H}_n^{\top})^{-1} \mathbf{Y}_n. \quad (7)$$

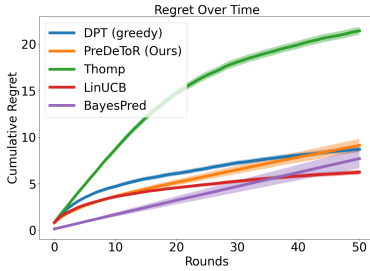


Figure 5: BayesPred Performance

The  $\widehat{\mu}$  in (7) represents the posterior mean vector averaged on all tasks. So if some action  $a \in [A]$  consistently yields high rewards in the pretraining data then  $\widehat{\mu}(a)$  has high value. Since the test distribution is the same as pretraining, this action on average will yield a high reward during test time.

We hypothesize that the PreDeToR is learning the reward correlation covariance matrix from the training data  $\mathcal{H}_{\text{train}}$  and acting greedily on it. To test this hypothesis, we consider the greedy BayesPred algorithm that first estimates  $\mathbf{S}_A$  from the pretraining data. It then uses the LMMSE estimator in Lemma 1 to calculate the posterior mean vector  $\widehat{\mu}$ , and then selects  $I_t = \arg \max_a \widehat{\mu}(a)$  at each round  $t$ . Note that BayesPred is a greedy algorithm that always

selects the most rewarding action (exploitation) without any exploration of sub-optimal actions. Also the BayesPred is an LMMSE estimator that leverages the linear reward structure and estimates the reward covariance matrix, and therefore can be interpreted as a lower bound to the regret of PreDeToR. The hypothesis that BayesPred is a lower bound to PreDeToR is supported by Figure 5. In Figure 5 the reward covariance matrix for BayesPred is estimated from the  $\mathcal{H}_{\text{train}}$  by first running the Thomp ( $\pi^w$ ). Observe that the BayesPred has a lower cumulative regret than PreDeToR and almost matches the regret of PreDeToR towards the end of the horizon. Also note that LinUCB has lower cumulative regret towards the end of horizon as it leverages the linear structure and the feature of the actions in selecting the next action.

## A.6 Empirical Study: Increasing number of Actions

In this section, we discuss the performance of PreDeToR when the number of actions is very high so that the weak demonstrator  $\pi^w$  does not have sufficient samples for each action. However, the number of tasks  $M_{\text{pre}} \gg A > n$ .

**Baselines:** We again implement the same baselines discussed in Section 4. The baselines are PreDeToR, PreDeToR- $\tau$ , DPT-greedy, AD, Thomp, and LinUCB.

**Outcomes:** We first discuss the main outcomes from our experimental results of introducing more actions than the horizon (or more dimensions than actions) during data collection and evaluation:

- (1) The PreDeToR ( $-\tau$ ) exploits the underlying latent structure and reward correlation between the different tasks even when  $A > n$  but  $M_{\text{pre}} \gg A$ .
- (2) The PreDeToR ( $-\tau$ ) has lower regret than its weak demonstrator even when it is trained on  $\mathcal{H}_{\text{train}} \subseteq \mathcal{D}_{\text{pre}}$ .
- (3) The PreDeToR ( $-\tau$ ) performance drops for complex non-linear bandit setting with increasing number of dimensions.

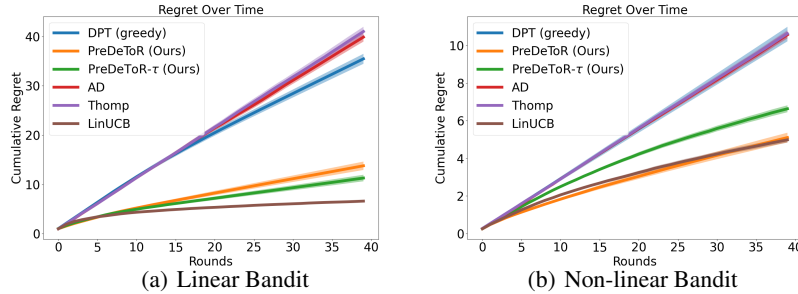


Figure 6: Testing the limit experiments. The horizontal axis is the number of rounds. Confidence bars show one standard error.

**Experimental Result:** We observe these outcomes in Figure 6. In Figure 6(a) we show the linear bandit setting for  $M_{\text{pre}} = 250000$ ,  $M_{\text{test}} = 200$ ,  $A = 100$ ,  $n = 50$  and  $d = 5$ . Again, the demonstrator  $\pi^w$  is the **Thomp** algorithm. We observe that **PreDeToR** ( $-\tau$ ) has lower cumulative regret than **DPT-greedy** and **AD**. Note that for any task  $m$  the **Thomp** will not be able to sample all the actions even once. The weak performance of **DPT-greedy** can be attributed to both short horizons and the inability to estimate the optimal action for such a short horizon  $n < A$ . The **AD** performs similar to the demonstrator **Thomp** because of its training. Observe that **PreDeToR** ( $-\tau$ ) has similar regret to **LinUCB** and lower regret than **Thomp** which also shows that **PreDeToR** is exploiting the latent linear structure of the underlying tasks. In Figure 6(b) we show the non-linear bandit setting for horizon  $n = 40$ ,  $M_{\text{pre}} = 200000$ ,  $A = 60$ ,  $d = 2$ , and  $|\mathcal{A}^{\text{inv}}| = 5$ . The demonstrator  $\pi^w$  is the **Thomp** algorithm. The training of **AD** ensures that it does not outperform the demonstrator **Thomp**. Again we observe that **PreDeToR** ( $-\tau$ ) has lower cumulative regret than **DPT-greedy**, **AD** and **LinUCB** which fails to perform well in this non-linear setting due to its algorithmic design.

### A.7 Empirical Study: Increasing Horizon

In this section, we discuss the performance of **PreDeToR** with respect to an increasing horizon for each task  $m \in [M]$ . However, note that the number of tasks  $M_{\text{pre}} \geq n$ . Note that **Lee et al. [2023]** studied linear bandit setting for  $n = 200$ . We study the setting up to a similar horizon scale.

**Baselines:** We again implement the same baselines discussed in Section 4. The baselines are **PreDeToR**, **PreDeToR- $\tau$** , **DPT-greedy**, **AD**, **Thomp**, and **LinUCB**.

**Outcomes:** We first discuss the main outcomes of our experimental results for increasing the horizon:

- (1) The **PreDeToR** ( $-\tau$ ) learns to exploit the underlying latent structure and reward correlation between the different tasks even when  $A \geq n$ ,  $M_{\text{pre}} \gg A$  with increasing horizon.
- (2) The **PreDeToR** ( $-\tau$ ) outperforms its weak demonstrator even when trained on  $\mathcal{H}_{\text{train}} \subseteq \mathcal{D}_{\text{pre}}$ .

**Experimental Result:** We observe these outcomes in Figure 7. In Figure 7 we show the linear bandit setting for  $M_{\text{pre}} = 150000$ ,  $M_{\text{test}} = 200$ ,  $A = 20$ ,  $n = \{20, 40, 60, 100, 120, 140, 200\}$  and  $d = 5$ . Again, the demonstrator  $\pi^w$  is the **Thomp** algorithm. We observe that **PreDeToR** ( $-\tau$ ) has lower cumulative regret than **DPT-greedy**, and **AD**. Note that for any task  $m$  for the horizon 20 the **Thomp** will be able to sample all the actions at most once. Observe from Figure 7(a), 7(b), 7(c), Figure 7(d), 7(e), 7(f) and 7(g) that **PreDeToR** ( $-\tau$ ) is closer to **LinUCB** and outperforms **Thomp** which also shows that **PreDeToR** ( $-\tau$ ) is learning the latent linear structure of the underlying tasks. In Figure 7(h) we plot the regret of all the baselines with respect to the increasing horizon. Again we see that **PreDeToR** ( $-\tau$ ) is closer to **LinUCB** and outperforms **DPT-greedy**, **AD** and **Thomp**. The training of **AD** ensures that it does not outperform the demonstrator **Thomp**. This shows that **PreDeToR** ( $-\tau$ ) is able to exploit the latent structure and reward correlation across the tasks for varying horizon length.

### A.8 Empirical Study: Increasing Dimension

In this section, we discuss the performance of **PreDeToR** with respect to an increasing dimension for each task  $m \in [M]$ . Again note that the number of tasks  $M_{\text{pre}} \gg A \geq n$ . Through this experiment, we want to evaluate the performance of **PreDeToR** and see how it exploits the underlying reward correlation when the horizon is small as well as for increasing dimensions.

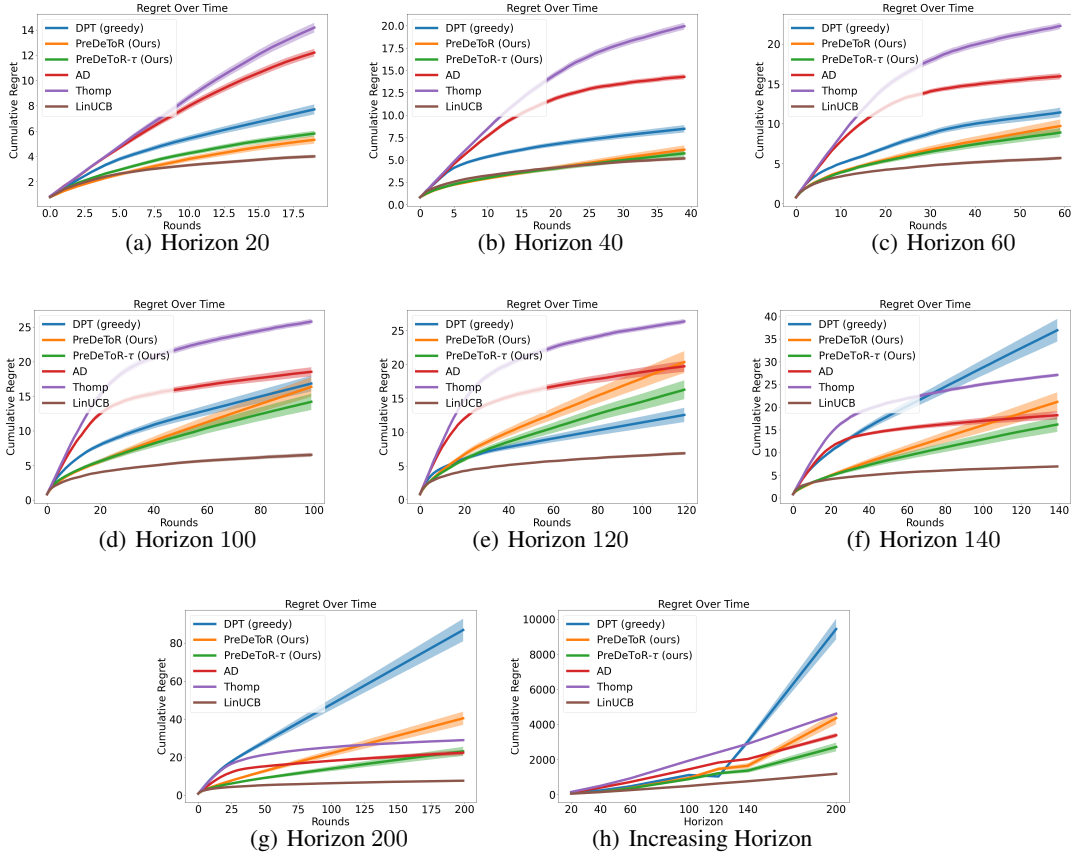


Figure 7: Experiment with increasing horizon. The y-axis shows the cumulative regret.

**Baselines:** We again implement the same baselines discussed in Section 4. The baselines are **PreDeToR**, **PreDeToR- $\tau$** , **DPT-greedy**, **AD**, **Thomp**, and **LinUCB**.

**Outcomes:** We first discuss the main outcomes of our experimental results for increasing the horizon:

- (1) The **PreDeToR (- $\tau$ )** learns to exploit the underlying latent structure and reward correlation between the different tasks even when  $A \geq n$  but  $M_{\text{pre}} \gg A$ .
- (2) The **PreDeToR (- $\tau$ )** has lower regret than its weak demonstrator even when trained on  $\mathcal{D}_{\text{train}} \subseteq \mathcal{D}_{\text{pre}}$ .
- (3) The **PreDeToR (- $\tau$ )** has lower regret than **LinUCB** for larger dimension.

**Experimental Result:** We observe these outcomes in Figure 7. In Figure 7 we show the linear bandit setting for horizon  $n = 20$ ,  $M_{\text{pre}} = 160000$ ,  $M_{\text{test}} = 200$ ,  $A = 20$ , and  $d = \{10, 20, 30, 40\}$ . Again, the demonstrator  $\pi^w$  is the **Thomp** algorithm. We observe that **PreDeToR (- $\tau$ )** has lower cumulative regret than **DPT-greedy**, **AD**. Note that for any task  $m$  for the horizon 20 the **Thomp** will be able to sample all the actions at most once. Observe from Figure 8(a), 8(b), 8(c), and 8(d) that **PreDeToR (- $\tau$ )** is closer to **LinUCB** and has lower regret than **Thomp** which also shows that **PreDeToR (- $\tau$ )** is exploiting the latent linear structure of the underlying tasks. In Figure 8(e) we plot the regret of all the baselines with respect to the increasing dimension. Again we see that **PreDeToR (- $\tau$ )** has lower regret than **DPT-greedy**, **AD** and **Thomp**. Observe that with increasing dimension **PreDeToR** is able to outperform **LinUCB**. This shows that the **PreDeToR (- $\tau$ )** is able to exploit reward correlation across tasks for varying dimensions.

## A.9 Empirical Study: Increasing Attention Heads

In this section, we discuss the performance of **PreDeToR** with respect to an increasing attention heads for the transformer model for the non-linear feedback model. Again note that the number of tasks



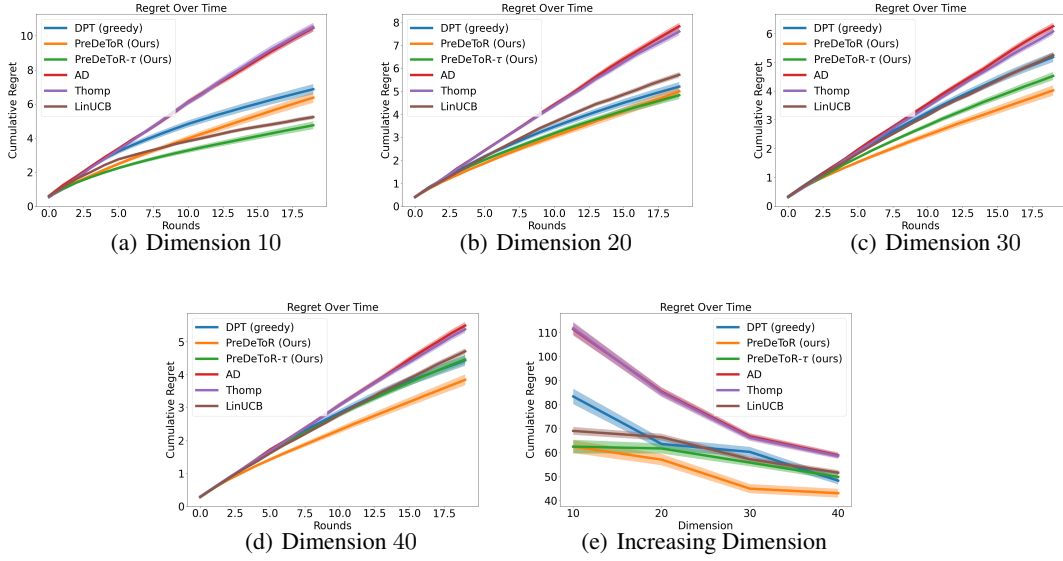


Figure 8: Experiment with increasing dimension. The y-axis shows the cumulative regret.

$M_{\text{pre}} \gg A \geq n$ . Through this experiment, we want to evaluate the performance of **PreDeToR** to exploit the underlying reward correlation when the horizon is small and understand the representative power of the transformer by increasing the attention heads. Note that we choose the non-linear feedback model and low data regime to leverage the representative power of the transformer.

**Baselines:** We again implement the same baselines discussed in Section 4. The baselines are **PreDeToR**, **PreDeToR- $\tau$** , **DPT-greedy**, **AD**, **Thomp**, and **LinUCB**.

**Outcomes:** We first discuss the main outcomes of our experimental results for increasing the horizon:

- (1) The **PreDeToR** ( $-\tau$ ) learns to exploit the underlying latent structure and reward correlation between the different tasks even when  $A \geq n$  but  $M_{\text{pre}} \gg A$ .
- (2) The **PreDeToR** ( $-\tau$ ) has lower regret than its weak demonstrator even when trained on  $\mathcal{D}_{\text{train}} \subseteq \mathcal{D}_{\text{pre}}$ .
- (3) The **PreDeToR** ( $-\tau$ ) has lower regret compared to **DPT-greedy**, **AD** with increasing attention heads.

**Experimental Result:** We observe these outcomes in Figure 9. In Figure 9 we show the non-linear bandit setting for horizon  $n = 20$ ,  $M_{\text{pre}} = 160000$ ,  $M_{\text{test}} = 200$ ,  $A = 20$ , heads =  $\{2, 4, 6, 8\}$  and  $d = 5$ . Again, the demonstrator  $\pi^w$  is the **Thomp** algorithm. We observe that **PreDeToR** ( $-\tau$ ) has lower cumulative regret than **DPT-greedy**, **AD**. Note that for any task  $m$  for the horizon 20 the **Thomp** will be able to sample all the actions at most once. Observe from Figure 9(a), 9(b), 9(c), and 9(d) that **PreDeToR** ( $-\tau$ ) has lower regret than **AD**, **Thomp** and **LinUCB** which also shows that **PreDeToR** ( $-\tau$ ) is exploiting the latent linear structure of the underlying tasks for the non-linear setting. The training of **AD** ensures that it does not outperform the demonstrator **Thomp**. In Figure 9(f) we plot the regret of all the baselines with respect to the increasing attention heads. Again we see that **PreDeToR** ( $-\tau$ ) regret decreases as we increase the attention heads.

## A.10 Empirical Study: Increasing Number of Tasks

In this section, we discuss the performance of **PreDeToR** with respect to the increasing number of tasks for the linear bandit setting. Again note that the number of tasks  $M_{\text{pre}} \gg A \geq n$ . Through this experiment, we want to evaluate the performance of **PreDeToR** to exploit the underlying reward correlation when the horizon is small and the number of tasks is changing. Finally, recall that when the horizon is small the weak demonstrator  $\pi^w$  does not have sufficient samples for each action. This leads to a poor approximation of the greedy action.

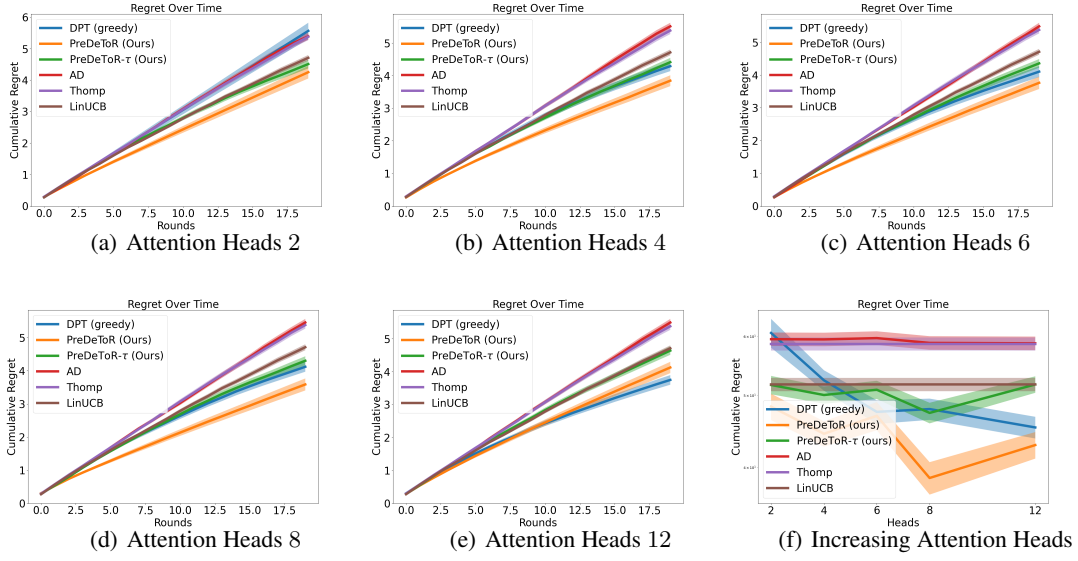


Figure 9: Experiment with increasing attention heads. The y-axis shows the cumulative regret.

**Baselines:** We again implement the same baselines discussed in Section 4. The baselines are **PreDeToR**, **PreDeToR- $\tau$** , **DPT-greedy**, **AD**, **Thomp**, and **LinUCB**.

**Outcomes:** We first discuss the main outcomes of our experimental results for increasing the horizon:

- (1) The **PreDeToR (- $\tau$ )** fails to exploit the underlying latent structure and reward correlation when the number of tasks is small.
- (2) As the number of tasks increases the **PreDeToR (- $\tau$ )** learns the latent structure and the underlying reward correlation.
- (3) The **PreDeToR (- $\tau$ )** has lower regret compared to **DPT-greedy**, **AD** with increasing number of tasks.

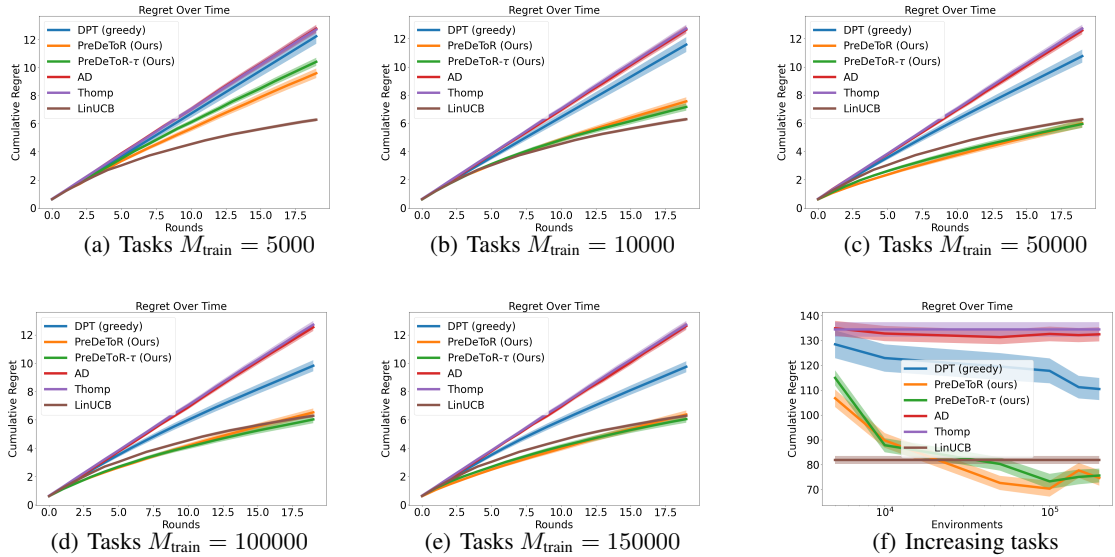


Figure 10: Experiment with an increasing number of tasks. The y-axis shows the cumulative regret.

**Experimental Result:** We observe these outcomes in Figure 10. In Figure 10 we show the linear bandit setting for horizon  $n = 20$ ,  $M_{\text{pre}} \in \{5000, 10000, 50000, 100000, 150000\}$ ,  $M_{\text{test}} = 200$ ,  $A = 20$ , and  $d = 40$ . Again, the demonstrator  $\pi^w$  is the **Thomp** algorithm. We observe that

**PreDeToR** ( $-\tau$ ), **AD** and **DPT-greedy** suffer more regret than the **LinUCB** when the number of tasks is small ( $M_{\text{train}} \in \{5000, 10000\}$  in Figure 10(a), and 10(b). However in Figure 10(c), 10(d), 10(e), and 10(f) we show that **PreDeToR** has lower regret than **Thomp** and matches **LinUCB**. This shows that **PreDeToR** ( $-\tau$ ) is exploiting the latent linear structure of the underlying tasks for the non-linear setting. Moreover, observe that as  $M_{\text{train}}$  increases the **PreDeToR** has lower cumulative regret than **DPT-greedy**, **AD**. Note that for any task  $m$  for the horizon 20 the **Thomp** will be able to sample all the actions at most once. Therefore **DPT-greedy** does not perform as well as **PreDeToR**. The training of **AD** ensures that it does not outperform the demonstrator **Thomp**. Finally, note that the result shows that **PreDeToR** ( $-\tau$ ) is able to exploit the reward correlation across the tasks better as the number of tasks increases.

### A.11 Exploration of **PreDeToR**( $-\tau$ )

In this section, we discuss the exploration of **PreDeToR** in the linear bandit setting discussed in Section 4. Recall that the linear bandit setting consist of horizon  $n = 25$ ,  $M_{\text{pre}} = 200000$ ,  $M_{\text{test}} = 200$ ,  $A = 10$ , and  $d = 2$ . The demonstrator  $\pi^w$  is the **Thomp** algorithm and we observe that **PreDeToR** ( $-\tau$ ) has lower cumulative regret than **DPT-greedy**, **AD** and matches the performance of **LinUCB**. Therefore **PreDeToR** ( $-\tau$ ) behaves almost optimally in this setting and so we analyze how **PreDeToR** conducts exploration for this setting.

**Outcomes:** We first discuss the main outcomes of our analysis of exploration in the low-data regime:

- (1) The **PreDeToR** ( $-\tau$ ) has a two phase exploration. In the first phase it explores with a strong prior over the training data. In the second phase, once the task data has been observed for a few rounds it switches to task-based exploration.
- (2) **PreDeToR** ( $-\tau$ ) samples the optimal action in each task more than **DPT-greedy**. **PreDeToR**( $-\tau$ ) considers a larger set of possible optimal action candidate set than **DPT-greedy**.

We first show in Figure 11(a) the training distribution of the optimal actions. For each bar, the frequency indicates the number of tasks where the action (shown in the x-axis) is the optimal action.

Then in Figure 11(b) we show how the sampling distribution of **DPT-greedy**, **PreDeToR** and **PreDeToR**- $\tau$  change in the first 10 and last 10 rounds for all the tasks where action 5 is optimal. To plot this graph we first sum over the individual pulls of the action taken by each algorithm over the first 10 and last 10 rounds. Then we average these counts over all test tasks where action 5 is optimal. From the figure Figure 11(b) we see that **PreDeToR**( $-\tau$ ) consistently pulls the action 5 more than **DPT-greedy**. It also explores other optimal actions like  $\{2, 3, 6, 7, 10\}$  but discards them quickly in favor of the optimal action 5 in these tasks. This shows that **PreDeToR** ( $-\tau$ ) only considers the optimal actions seen from the training data. Once sufficient observation have been observed for the task it switches to task-based exploration and samples the optimal action more than **DPT-greedy**.

Finally, we plot the feasible action set considered by **DPT-greedy**, **PreDeToR**, and **PreDeToR**- $\tau$  in Figure 11(c). To plot this graph again we consider the test tasks where the optimal action is 5. Then we count the number of distinct actions that are taken from round  $t$  up until horizon  $n$ . Finally we average this over all the considered tasks where the optimal action is 5. We call this the candidate action set considered by the algorithm. From the Figure 11(c) we see that **DPT-greedy** explores the least and gets stuck with few actions quickly (by round 10). Note that the actions **DPT-greedy** samples are sub-optimal and so it suffers a high cumulative regret (see Figure 1(a)). **PreDeToR** explore slightly more than **DPT-greedy**, but **PreDeToR**- $\tau$  explores the most.

### A.12 Exploration of **PreDeToR**( $-\tau$ ) in New Arms Setting

In this section, we discuss the exploration of **PreDeToR** ( $-\tau$ ) in the linear and non-linear new arms bandit setting discussed in Section 5. Recall that we consider the linear bandit setting of horizon  $n = 50$ ,  $M_{\text{pre}} = 200000$ ,  $M_{\text{test}} = 200$ ,  $A = 20$ , and  $d = 5$ . Here during data collection and during collecting the test data, we randomly select one new action from  $\mathbb{R}^d$  for each task  $m$ . So the number of invariant actions is  $|\mathcal{A}^{\text{inv}}| = 19$ .

**Outcomes:** We first discuss the main outcomes of our analysis of exploration in the low-data regime:

- (1) The **PreDeToR** ( $-\tau$ ) is robust to changes when the number of changing arms is small. It samples the optimal action in each task more than **DPT-greedy**.

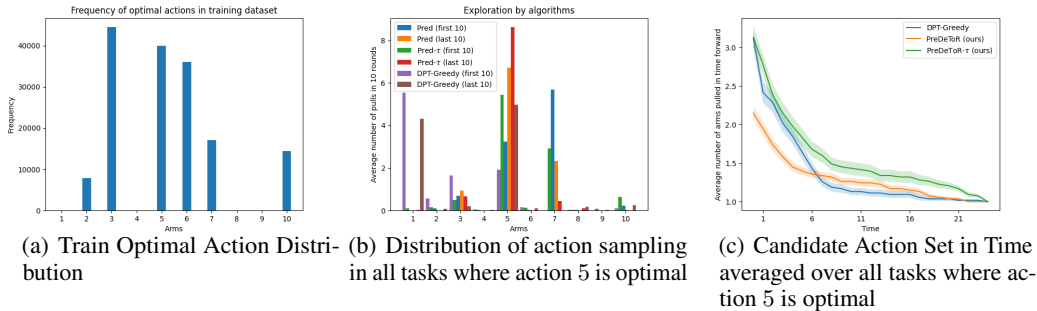


Figure 11: Exploration Analysis of  $\text{PreDeToR}(-\tau)$

(2) When the number of in-variant actions is small then all algorithms  $\text{PreDeToR}$ ,  $\text{PreDeToR}-\tau$ , and  $\text{AD}$  sample the optimal action very less. This shows that the latent shared structure across the tasks is very important.

We first show in Figure 12(a) the training distribution of the optimal actions. For each bar, the frequency indicates the number of tasks where the action (shown in the x-axis) is the optimal action.

Then in Figure 12(b) we show how the sampling distribution of  $\text{DPT-greedy}$ ,  $\text{PreDeToR}$  and  $\text{PreDeToR}-\tau$  change in the first 10 and last 10 rounds for all the tasks where action 17 is optimal. We plot this graph the same way as discussed in Appendix A.11. From the figure Figure 12(b) we see that  $\text{PreDeToR}(-\tau)$  consistently pulls the action 17 more than  $\text{DPT-greedy}$ . It also explores other optimal actions like  $\{1, 2, 3, 8, 9, 15\}$  but discards them quickly in favor of the optimal action 17 in these tasks.

Finally, we plot the feasible action set considered by  $\text{DPT-greedy}$ ,  $\text{PreDeToR}$ , and  $\text{PreDeToR}-\tau$  in Figure 12(c). To plot this graph again we consider the test tasks where the optimal action is 17. Then we count the number of distinct actions that are taken from round  $t$  up until horizon  $n$ . Finally we average this over all the considered tasks where the optimal action is 17. We call this the candidate action set considered by the algorithm. From the Figure 12(c) we see that  $\text{PreDeToR}-\tau$  explores more than  $\text{PreDeToR}$  in this setting.

We also show how the prediction error of the optimal action by  $\text{PreDeToR}$  compared to  $\text{LinUCB}$  in this 1 new arm linear bandit setting. In Figure 13(a) we first show how the 20 actions are distributed in the  $M_{\text{test}} = 200$  test tasks. In Figure 13(a) for each bar, the frequency indicates the number of tasks where the action (shown in the x-axis) is the optimal action. Then in Figure 13(b) we show the prediction error of  $\text{PreDeToR}(-\tau)$  for each task  $m \in [M_{\text{test}}]$ . The prediction error is calculated the same way as stated in Section 5 From the Figure 13(b) we see that for most actions the prediction error of  $\text{PreDeToR}(-\tau)$  is closer to  $\text{LinUCB}$  showing that the introduction of 1 new action does not alter the prediction error much. Note that  $\text{LinUCB}$  estimates the empirical mean directly from the test task, whereas  $\text{PreDeToR}$  has a strong prior based on the training data. Therefore we see that  $\text{PreDeToR}$  is able to estimate the reward of the optimal action quite well from the training dataset  $\mathcal{D}_{\text{pre}}$ .

We now consider the setting where the number of invariant actions is  $|\mathcal{A}^{\text{inv}}| = 15$ . We again show in Figure 14(a) the training distribution of the optimal actions. For each bar, the frequency indicates the number of tasks where the action (shown in the x-axis) is the optimal action. Then in Figure 14(b) we show how the sampling distribution of  $\text{DPT-greedy}$ ,  $\text{PreDeToR}$  and  $\text{PreDeToR}-\tau$  change in the first 10 and last 10 rounds for all the tasks where action 17 is optimal. We plot this graph the same way as discussed in Appendix A.11. From the figure Figure 14(b) we see that none of the algorithms  $\text{PreDeToR}$ ,  $\text{PreDeToR}-\tau$ ,  $\text{DPT-greedy}$  consistently pulls the action 17 more than other actions. This shows that the common underlying actions across the tasks matter for learning the exploration.

Finally, we plot the feasible action set considered by  $\text{DPT-greedy}$ ,  $\text{PreDeToR}$ , and  $\text{PreDeToR}-\tau$  in Figure 14(c). To plot this graph again we consider the test tasks where the optimal action is 17. We build the candidate set the same way as before. From the Figure 14(c) we see that none of the three

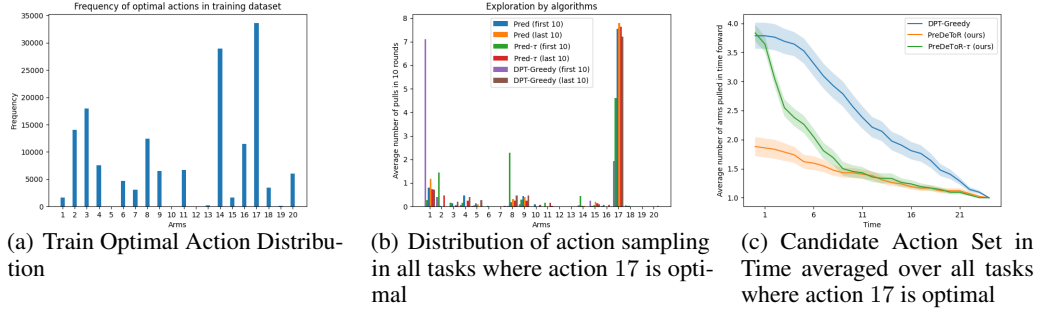


Figure 12: Exploration Analysis of  $\text{PreDeToR}(-\tau)$  in linear 1 new arm setting

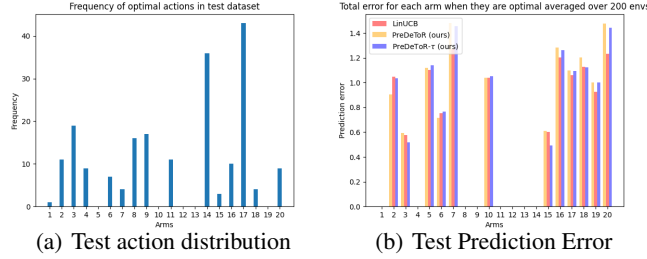


Figure 13: Prediction error of  $\text{PreDeToR}(-\tau)$  in linear 1 new arm setting

algorithms  $\text{DPT-greedy}$ ,  $\text{PreDeToR}$ ,  $\text{PreDeToR}(-\tau)$ , is able to sample the optimal action 17 sufficiently high number of times.

We also show how the prediction error of the optimal action by  $\text{PreDeToR}$  compared to  $\text{LinUCB}$  in this 1 new arm linear bandit setting. In Figure 15(a) we first show how the 20 actions are distributed in the  $M_{\text{test}} = 200$  test tasks. In Figure 15(a) for each bar, the frequency indicates the number of tasks where the action (shown in the x-axis) is the optimal action. Then in Figure 15(b) we show the prediction error of  $\text{PreDeToR}(-\tau)$  for each task  $m \in [M_{\text{test}}]$ . The prediction error is calculated the same way as stated in Section 5. From the Figure 15(b) we see that for most actions the prediction error is higher than  $\text{LinUCB}$  showing that the introduction of 5 new actions (and thereby decreasing the invariant action set) significantly alters the prediction error.

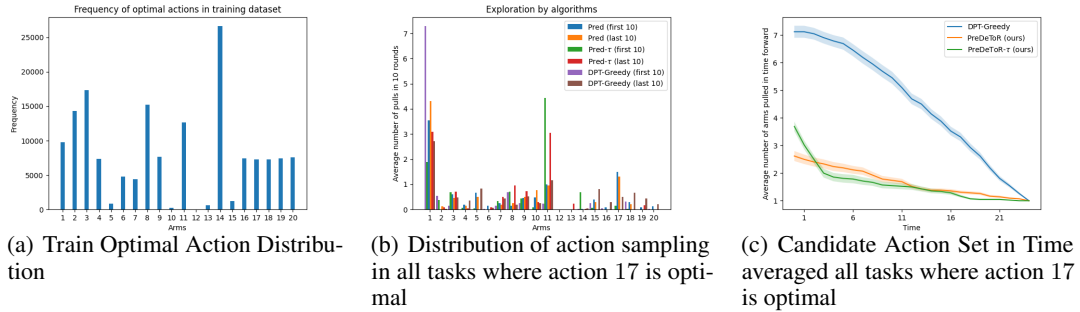


Figure 14: Exploration Analysis of  $\text{PreDeToR}(-\tau)$  in linear 5 new arm setting

### A.13 Data Collection Analysis

In this section, we analyze the performance of  $\text{PreDeToR}$ ,  $\text{PreDeToR}(-\tau)$ ,  $\text{DPT-greedy}$ ,  $\text{AD}$ ,  $\text{Thomp}$ , and  $\text{LinUCB}$  when the weak demonstrator  $\pi^w$  is  $\text{Thomp}$ ,  $\text{LinUCB}$ , or  $\text{Uniform}$ . We again consider the linear bandit setting discussed in Section 4. Recall that the linear bandit setting consist of horizon  $n = 25$ ,  $M_{\text{pre}} = 200000$ ,  $M_{\text{test}} = 200$ ,  $A = 10$ , and  $d = 2$ . Finally, we show the cumulative regret by

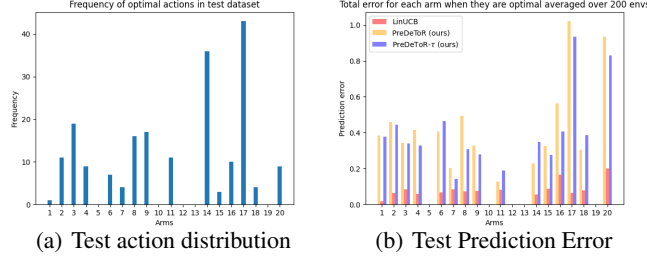


Figure 15: Prediction error of  $\text{PreDeToR}(-\tau)$  in linear 1 new arm setting

the above baselines in Figure 16(a), 16(b), and 16(c) when data is collected through  $\text{Thomp}$ ,  $\text{LinUCB}$ , and  $\text{Uniform}$  respectively.

**Outcomes:** We first discuss the main outcomes of our experimental results for different data collection:

- (1) The  $\text{PreDeToR}(-\tau)$  excels in exploiting the underlying latent structure and reward correlation when the data diversity is high.
- (2) The  $\text{PreDeToR}(-\tau)$  fails to exploit the underlying latent structure and reward correlation when the data diversity is less.
- (3) The  $\text{PreDeToR}(-\tau)$  has lower regret compared to  $\text{DPT-greedy}$  in all settings.  $\text{AD}$  outperforms  $\text{PreDeToR}(-\tau)$  when data is collected by  $\text{LinUCB}$ .

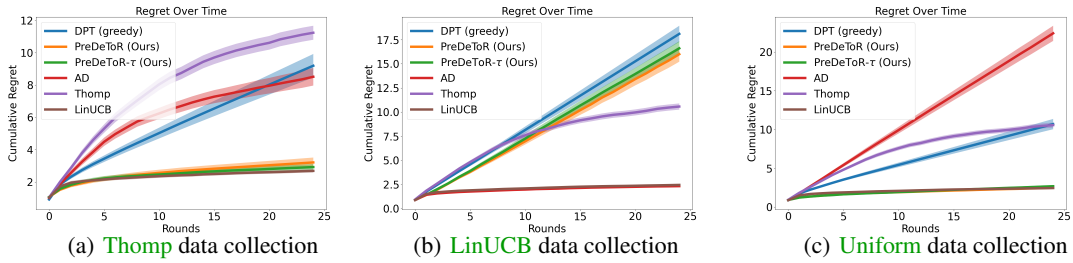


Figure 16: Data Collection with various algorithms and Performance analysis

**Experimental Result:** We observe these outcomes in Figure 16. In Figure 16(a) we see that the  $A$ -actioned  $\text{Thomp}$  is explorative enough as it does not explore with the knowledge of feature representation. So it pulls the sub-optimal actions sufficiently high number of times before discarding them in favor of the optimal action. Therefore the training data is diverse enough so that  $\text{PreDeToR}(-\tau)$  can predict the reward vectors for actions sufficiently well. Consequently,  $\text{PreDeToR}(-\tau)$  almost matches the  $\text{LinUCB}$  algorithm. Both  $\text{DPT-greedy}$  and  $\text{AD}$  perform poorly in this setting.

In Figure 16(b) we see that the  $\text{LinUCB}$  algorithm is not explorative enough as it explores with the knowledge of feature representation and quickly discards the sub-optimal actions in favor of the optimal action. Therefore the training data is not diverse enough so that  $\text{PreDeToR}(-\tau)$  is not able to correctly predict the reward vectors for actions. Note that  $\text{DPT-greedy}$  also performs poorly in this setting when it is not provided with the optimal action information during training. The  $\text{AD}$  matches the performance of its demonstrator  $\text{LinUCB}$  because of its training procedure of predicting the next action of the demonstrator.

Finally, in Figure 16(c) we see that the  $A$ -armed  $\text{Uniform}$  is fully explorative as it does not intend to minimize regret (as opposed to  $\text{Thomp}$ ) and does not explore with the knowledge of feature representation. Therefore the training data is very diverse which results in  $\text{PreDeToR}(-\tau)$  being able to predict the reward vectors for actions very well. Consequently,  $\text{PreDeToR}(-\tau)$  perfectly matches the  $\text{LinUCB}$  algorithm. Note that  $\text{AD}$  performs the worst as it matches the performance of its demonstrator whereas the performance of  $\text{DPT-greedy}$  suffers due to the lack of information on the optimal action during training.

## A.14 Empirical Validation of Theoretical Result

In this section, we empirically validate the theoretical result proved in Section 6. We again consider the linear bandit setting discussed in Section 4. Recall that the linear bandit setting consist of horizon  $n = 25$ ,  $M_{\text{pre}} = \{100000, 200000\}$ ,  $M_{\text{test}} = 200$ ,  $A = 10$ , and  $d = 2$ . The demonstrator  $\pi^w$  is the **Thomp** algorithm and we observe that **PreDeToR** ( $-\tau$ ) has lower cumulative regret than **DPT-greedy**, **AD** and matches the performance of **LinUCB**.

**Baseline (LinUCB- $\tau$ ):** We define soft LinUCB (**LinUCB- $\tau$** ) as follows: At every round  $t$  for task  $m$ , it calculates the ucb value  $B_{m,a,t}$  for each action  $\mathbf{x}_{m,a} \in \mathcal{X}$  such that  $B_{m,a,t} = \mathbf{x}_{m,a}^\top \hat{\boldsymbol{\theta}}_{m,t-1} + \alpha \|\mathbf{x}_{m,a}\|_{\boldsymbol{\Sigma}_{m,t-1}^{-1}}$  where  $\alpha > 0$  is a constant and  $\hat{\boldsymbol{\theta}}_{m,t}$  is the estimate of the model parameter  $\boldsymbol{\theta}_{m,*}$  at round  $t$ . Here,  $\boldsymbol{\Sigma}_{m,t-1} = \sum_{s=1}^{t-1} \mathbf{x}_{m,s} \mathbf{x}_{m,s}^\top + \lambda \mathbf{I}_d$  is the data covariance matrix or the arms already tried. Then it chooses  $I_t \sim \text{softmax}_a^\tau(B_{m,a,t})$ , where  $\text{softmax}_a^\tau(\cdot) \in \Delta^A$  denotes a softmax distribution over the actions and  $\tau$  is a temperature parameter (See Section 4 for definition of  $\text{softmax}_a^\tau(\cdot)$ ).

**Outcomes:** We first discuss the main outcomes of our experimental results:

- (1) The **PreDeToR** ( $-\tau$ ) excels in predicting the rewards for test tasks when the number of training (source) tasks is large.
- (2) The **PreDeToR** ( $-\tau$ ) has a poor prediction of the rewards for test tasks when the number of training (source) tasks is small.

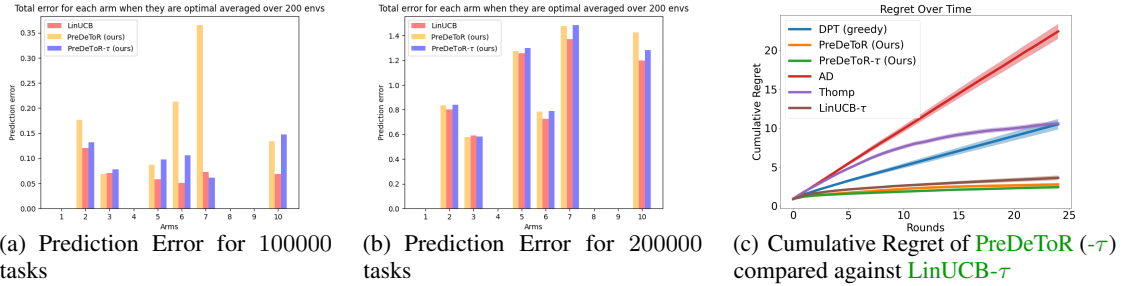


Figure 17: Empirical validation of theoretical analysis

**Experimental Result:** These findings are reported in Figure 17. In Figure 17(a) we show the prediction error of **PreDeToR** ( $-\tau$ ) for each task  $m \in [M_{\text{test}}]$ . The prediction error is calculated as  $(\hat{\mu}_{m,n,*}(a) - \mu_{m,*}(a))^2$  where  $\hat{\mu}_{m,n,*}(a) = \max_a \hat{\boldsymbol{\theta}}_{m,n}^\top \mathbf{x}_m(a)$  is the empirical mean at the end of round  $n$ , and  $\mu_{m,*}(a) = \max_a \boldsymbol{\theta}_{m,*}^\top \mathbf{x}_m(a)$  is the true mean of the optimal action in task  $m$ . Then we average the prediction error for the action  $a \in [A]$  by the number of times the action  $a$  is the optimal action in some task  $m$ . We see that when the source tasks are 100000 the reward prediction falls short of **LinUCB** prediction for all actions except action 2.

In Figure 17(b) we again show the prediction error of **PreDeToR** ( $-\tau$ ) for each task  $m \in [M_{\text{test}}]$  when the source tasks are 200000. Note that in both these settings, we kept the horizon  $n = 25$ , and the same set of actions. We now observe that the reward prediction almost matches **LinUCB** prediction in almost all the optimal actions.

In Figure 17(c) we compare **PreDeToR** ( $-\tau$ ) against **LinUCB- $\tau$**  and show that they almost match in the linear bandit setting discussed in Section 4 when the source tasks are 100000.

## A.15 Empirical Study: Offline Performance

In this section, we discuss the offline performance of **PreDeToR** when the number of tasks  $M_{\text{pre}} \gg A \geq n$ .

We first discuss how **PreDeToR** ( $-\tau$ ) is modified for the offline setting. In the offline setting, the **PreDeToR** first samples a task  $m \sim \mathcal{T}_{\text{test}}$ , then the test dataset  $\mathcal{H}_m \sim \mathcal{D}_{\text{test}}(\cdot|m)$ . Then **PreDeToR** and

**PreDeToR- $\tau$**  act similarly to the online setting, but based on the entire offline dataset  $\mathcal{H}_m$ . The full pseudocode of **PreDeToR** is in Algorithm 2.

---

**Algorithm 2** Pre-trained Decision Transformer with Reward Estimation (**PreDeToR**)

---

- 1: **Collecting Pretraining Dataset**
- 2: Initialize empty pretraining dataset  $\mathcal{H}_{\text{train}}$
- 3: **for**  $i$  in  $[M_{\text{pre}}]$  **do**
- 4:   Sample task  $m \sim \mathcal{T}_{\text{pre}}$ , in-context dataset  $\mathcal{H}_m \sim \mathcal{D}_{\text{pre}}(\cdot|m)$  and add this to  $\mathcal{H}_{\text{train}}$ .
- 5: **end for**
- 6: **Pretraining model on dataset**
- 7: Initialize model  $\text{TF}_{\Theta}$  with parameters  $\Theta$
- 8: **while** not converged **do**
- 9:   Sample  $\mathcal{H}_m$  from  $\mathcal{H}_{\text{train}}$  and predict  $\hat{r}_{m,t}$  for action  $(I_{m,t})$  for all  $t \in [n]$
- 10:   Compute loss in (3) with respect to  $r_{m,t}$  and backpropagate to update model parameter  $\Theta$ .
- 11: **end while**
- 12: **Offline test-time deployment**
- 13: Sample unknown task  $m \sim \mathcal{T}_{\text{test}}$ , sample dataset  $\mathcal{H}_m \sim \mathcal{D}_{\text{test}}(\cdot|m)$
- 14: Use  $\text{TF}_{\Theta}$  on  $m$  at round  $t$  to choose

$$I_t \begin{cases} = \arg \max_{a \in \mathcal{A}} \text{TF}_{\Theta}(\hat{r}_{m,t}(a) | \mathcal{H}_m), & \text{PreDeToR} \\ \sim \text{softmax}_a^{\tau} \text{TF}_{\Theta}(\hat{r}_{m,t}(a) | \mathcal{H}_m), & \text{PreDeToR-}\tau \end{cases}$$

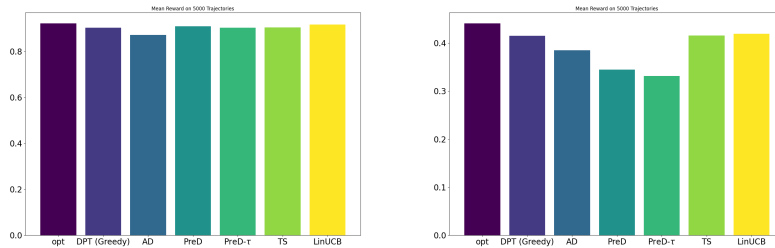

---

Recall that  $\mathcal{D}_{\text{test}}$  denote a distribution over all possible interactions that can be generated by  $\pi^w$  during test time. For offline testing, first, a test task  $m \sim \mathcal{T}_{\text{test}}$ , and then an in-context test dataset  $\mathcal{H}_m$  is collected such that  $\mathcal{H}_m \sim \mathcal{D}_{\text{test}}(\cdot|m)$ . Observe from Algorithm 2 that in the offline setting, **PreDeToR** first samples a task  $m \sim \mathcal{T}_{\text{test}}$ , and then a test dataset  $\mathcal{H}_m \sim \mathcal{D}_{\text{test}}(\cdot|m)$  and acts greedily. Crucially in the offline setting the **PreDeToR** does not add the observed reward  $r_t$  at round  $t$  to the dataset. Through this experiment, we want to evaluate the performance of **PreDeToR** to learn the underlying latent structure and reward correlation when the horizon is small. Finally, recall that when the horizon is small the weak demonstrator  $\pi^w$  does not have sufficient samples for each action. This leads to a poor approximation of the greedy action.

**Baselines:** We again implement the same baselines discussed in Section 4. The baselines are **PreDeToR**, **PreDeToR- $\tau$** , **DPT-greedy**, **AD**, **Thomp**, and **LinUCB**. During test time evaluation for offline setting the **DPT** selects  $I_t = \hat{a}_{m,t,*}$  where  $\hat{a}_{m,t,*} = \arg \max_a \text{TF}_{\Theta}(a|\mathcal{H}_m^t)$  is the predicted optimal action.

**Outcomes:** We first discuss the main outcomes of our experimental results for increasing the horizon:

- (1) The **PreDeToR** performs comparably with respect to cumulative regret against **DPT-greedy** both for the long horizon and the short horizon setting.
- (2) The **PreDeToR** performs comparably with respect to cumulative regret against **DPT-greedy** both for the linear and the non-linear bandit setting.
- (3) The **PreDeToR** and **DPT-greedy** has comparable regret to the weak demonstrator **Thomp** and **LinUCB** in the offline setting.



(a) Offline for Linear setting

(b) Offline for Non-linear setting

Figure 18: Offline experiment. The y-axis shows the cumulative reward.



**Experimental Result:** We observe these outcomes in Figure 18. In Figure 18 we show the linear bandit setting for horizon  $n = 20$ ,  $M_{\text{pre}} = 200000$ ,  $M_{\text{test}} = 5000$ ,  $A = 20$ , and  $d = 5$  for the low data regime. Again, the demonstrator  $\pi^w$  is the **Thomp** algorithm. We observe that **PreDeToR** ( $-\tau$ ) has comparable cumulative regret to **DPT-greedy**. Note that for any task  $m$  for the horizon  $n = 20$  the **Thomp** will be able to sample all the actions at most once. In the non-linear setting of Figure 18(b) the  $n = 40$ ,  $M_{\text{pre}} = 100000$ ,  $A = 6$ ,  $d = 2$ . Observe that in all of these results, the performance of **PreDeToR** ( $-\tau$ ) is comparable with respect to cumulative regret against **DPT-greedy**.

## B Theoretical Analysis

### B.1 Proof of Lemma 1

*Proof.* The learner collects  $n$  rounds of data following  $\pi^w$ . The weak demonstrator  $\pi^w$  only observes the  $\{I_t, r_t\}_{t=1}^n$ . Recall that  $N_n(a)$  denotes the total number of times the action  $a$  is sampled for  $n$  rounds. Define the matrix  $\mathbf{H}_n \in \mathbb{R}^{n \times A}$  where the  $t$ -th row represents the action sampled at round  $t \in [n]$ . The  $t$ -th row is a one-hot vector with 1 as the  $a$ -th component in the vector for  $a \in [A]$ . Then define the reward vector  $\mathbf{Y}_n \in \mathbb{R}^n$  as the reward vector where the  $t$ -th component is the observed reward for the action  $I_t$  for  $t \in [n]$ . Finally define the diagonal matrix  $\mathbf{D}_A \in \mathbb{R}^{A \times A}$  as in (6) and the estimated reward covariance matrix as  $\mathbf{S}_A \in \mathbb{R}^{A \times A}$  such that  $\mathbf{S}_A(a, a') = \hat{\mu}_n(a)\hat{\mu}_n(a')$ . This matrix captures the reward correlation between the pairs of actions  $a, a' \in [A]$ .

Assume  $\mu \sim \mathcal{N}(0, \mathbf{S}_*)$  where  $\mathbf{S}_* \in \mathbb{R}^{A \times A}$ . Then the observed mean vector  $\mathbf{Y}_n$  is

$$\mathbf{Y}_n = \mathbf{H}_n \mu + \mathbf{H}_n \mathbf{D}_A^{1/2} \eta_n$$

where,  $\eta_n$  is the noise vector over the  $[n]$  training data. Then the posterior mean of  $\hat{\mu}$  by Gauss Markov Theorem [Johnson et al., 2002] is given by

$$\hat{\mu} = \mathbf{S}_* \mathbf{H}_n^\top (\mathbf{H}_n (\mathbf{S}_* + \mathbf{D}_A) \mathbf{H}_n^\top)^{-1} \mathbf{Y}_n. \quad (8)$$

However, the learner does not know the true reward co-variance matrix. Hence it needs to estimate the  $\mathbf{S}_*$  from the observed data. Let the estimate be denoted by  $\mathbf{S}_A$ .

**Assumption B.1.** We assume that  $\pi^w$  is sufficiently exploratory so that each action is sampled at least once.

The Assumption B.1 ensures that the matrix  $(\sigma_\theta^2 \mathbf{H}_n (\mathbf{S}_A + \mathbf{D}_A) \mathbf{H}_n^\top)^{-1}$  is invertible. Under Assumption B.1, plugging the estimate  $\mathbf{S}_A$  back in (8) shows that the average posterior mean over all the tasks is

$$\hat{\mu} = \mathbf{S}_A \mathbf{H}_n^\top (\mathbf{H}_n (\mathbf{S}_A + \mathbf{D}_A) \mathbf{H}_n^\top)^{-1} \mathbf{Y}_n. \quad (9)$$

The claim of the lemma follows.  $\square$

## C Generalization and Transfer Learning Proof for **PreDeToR**

### C.1 Generalization Proof

Alg is the space of algorithms induced by the transformer  $\text{TF}_\Theta$ .

**Theorem C.1. (**PreDeToR** risk)** Suppose error stability Assumption 6.1 holds and assume loss function  $\ell(\cdot, \cdot)$  is  $C$ -Lipschitz for all  $r_t \in [0, B]$  and horizon  $n \geq 1$ . Let  $\widehat{\text{TF}}$  be the empirical solution of (ERM) and  $\mathcal{N}(\mathcal{A}, \rho, \epsilon)$  be the covering number of the algorithm space Alg following Definition C.2 and C.3. Then with probability at least  $1 - 2\delta$ , the excess Multi-task learning (MTL) risk of **PreDeToR**- $\tau$  is bounded by

$$\mathcal{R}_{\text{MTL}}(\widehat{\text{TF}}) \leq 4 \frac{C}{\sqrt{nM}} + 2(B + K \log n) \sqrt{\frac{\log(\mathcal{N}(\text{Alg}, \rho, \epsilon)/\delta)}{cnM}}$$

where,  $\mathcal{N}(\text{Alg}, \rho, \epsilon)$  is the covering number of transformer  $\widehat{\text{TF}}$ .

*Proof.* We consider a meta-learning setting. Let  $M$  source tasks are i.i.d. sampled from a task distribution  $\mathcal{T}$ , and let  $\widehat{\text{TF}}$  be the empirical Multitask (MTL) solution. Define  $\mathcal{H}_{\text{all}} = \bigcup_{m=1}^M \mathcal{H}_m$ . We drop the  $\Theta, \mathbf{r}$  from transformer notation  $\text{TF}^{\mathbf{r}, \Theta}$  as we keep the architecture fixed as in [Lin et al. \[2023\]](#). Note that this transformer predicts a reward vector over the actions. To be more precise we denote the reward predicted by the transformer at round  $t$  after observing history  $\mathcal{H}_m^{t-1}$  and then sampling the action  $a_{mt}$  as  $\text{TF}(\widehat{r}_{mt}(a_{mt}) | \mathcal{H}_m^{t-1}, a_{mt})$ . Define the training risk

$$\widehat{\mathcal{L}}_{\mathcal{H}_{\text{all}}}(\text{TF}) = \frac{1}{nM} \sum_{m=1}^M \sum_{t=1}^n \ell(r_{mt}(a_{mt}), \text{TF}(\widehat{r}_{mt}(a_{mt}) | \mathcal{H}_m^{t-1}, a_{mt}))$$

and the test risk

$$\mathcal{L}_{\text{MTL}}(\text{TF}) = \mathbb{E} \left[ \widehat{\mathcal{L}}_{\mathcal{H}_{\text{all}}}(\text{TF}) \right].$$

Define empirical risk minima  $\widehat{\text{TF}} = \arg \min_{\text{TF} \in \text{Alg}} \widehat{\mathcal{L}}_{\mathcal{H}_{\text{all}}}(\text{TF})$  and population minima

$$\text{TF}^* = \arg \min_{\text{TF} \in \text{Alg}} \mathcal{L}_{\text{MTL}}(\text{TF})$$

In the following discussion, we drop the subscripts MTL and  $\mathcal{H}_{\text{all}}$ . The excess MTL risk is decomposed as follows:

$$\begin{aligned} \mathcal{R}_{\text{MTL}}(\widehat{\text{TF}}) &= \mathcal{L}(\widehat{\text{TF}}) - \mathcal{L}(\text{TF}^*) \\ &= \underbrace{\mathcal{L}(\widehat{\text{TF}}) - \widehat{\mathcal{L}}(\widehat{\text{TF}})}_a + \underbrace{\widehat{\mathcal{L}}(\widehat{\text{TF}}) - \widehat{\mathcal{L}}(\text{TF}^*)}_b + \underbrace{\widehat{\mathcal{L}}(\text{TF}^*) - \mathcal{L}(\text{TF}^*)}_c. \end{aligned}$$

Since  $\widehat{\text{TF}}$  is the minimizer of empirical risk, we have  $b \leq 0$ .

**Step 1: (Concentration bound  $|\mathcal{L}(\text{TF}) - \widehat{\mathcal{L}}(\text{TF})|$  for a fixed  $\text{TF} \in \text{Alg}$ )** Define the test/train risks of each task as follows:

$$\widehat{\mathcal{L}}_m(\text{TF}) := \frac{1}{n} \sum_{t=1}^n \ell(r_{mt}(a_{mt}), \text{TF}(\widehat{r}_{mt}(a_{mt}) | \mathcal{H}_m^{t-1}, a_{mt})), \quad \text{and}$$

$$\mathcal{L}_m(\text{TF}) := \mathbb{E}_{\mathcal{H}_m} \left[ \widehat{\mathcal{L}}_m(\text{TF}) \right] = \mathbb{E}_{\mathcal{H}_m} \left[ \frac{1}{n} \sum_{t=1}^n \ell(r_{mt}(a_{mt}), \text{TF}(\widehat{r}_{mt}(a_{mt}) | \mathcal{H}_m^{t-1}, a_{mt})) \right], \quad \forall m \in [M].$$

Define the random variables  $X_{m,t} = \mathbb{E} \left[ \widehat{\mathcal{L}}_t(\text{TF}) | \mathcal{H}_m^t \right]$  for  $t \in [n]$  and  $m \in [M]$ , that is,  $X_{m,t}$  is the expectation over  $\widehat{\mathcal{L}}_t(\text{TF})$  given training sequence  $\mathcal{H}_m^t = \{(a_{mt'}, r_{mt'})\}_{t'=1}^t$  (which are the filtrations). With this, we have that  $X_{m,n} = \mathbb{E} \left[ \widehat{\mathcal{L}}_m(\text{TF}) | \mathcal{H}_m^n \right] = \widehat{\mathcal{L}}_m(\text{TF})$  and  $X_{m,0} = \mathbb{E} \left[ \widehat{\mathcal{L}}_m(\text{TF}) \right] = \mathcal{L}_m(\text{TF})$ . More generally,  $(X_{m,0}, X_{m,1}, \dots, X_{m,n})$  is a martingale sequence since, for every  $m \in [M]$ , we have that  $\mathbb{E} [X_{m,i} | \mathcal{H}_m^{i-1}] = X_{m,i-1}$ . For notational simplicity, in the following discussion, we omit the subscript  $m$  from  $a, r$  and  $\mathcal{H}$  as they will be clear from the left-hand-side variable  $X_{m,t}$ . We have that

$$\begin{aligned} X_{m,t} &= \mathbb{E} \left[ \frac{1}{n} \sum_{t'=1}^n \ell(r_{t'}, \text{TF}(\widehat{r}_{t'} | \mathcal{H}^{t'-1}, a_{t'})) \middle| \mathcal{H}^t \right] \\ &= \frac{1}{n} \sum_{t'=1}^t \ell(r_{t'}, \text{TF}(\widehat{r}_{t'} | \mathcal{H}^{t'-1}, a_{t'})) + \frac{1}{n} \sum_{t'=t+1}^n \mathbb{E} \left[ \ell(r_{t'}, \text{TF}(\widehat{r}_{t'} | \mathcal{H}^{t'-1}, a_{t'})) \middle| \mathcal{H}^t \right] \end{aligned}$$

Using the similar steps as in [Li et al. \[2023\]](#) we can show that

$$|X_{m,t} - X_{m,t-1}| \stackrel{(a)}{\leq} \frac{B}{n} + \sum_{t'=t+1}^n \frac{K}{t'n} \leq \frac{B + K \log n}{n}.$$

where, (a) follows by using the fact that loss function  $\ell(\cdot, \cdot)$  is bounded by  $B$ , and error stability assumption.

Recall that  $|\mathcal{L}_m(\text{TF}) - \widehat{\mathcal{L}}_m(\text{TF})| = |X_{m,0} - X_{m,n}|$  and for every  $m \in [M]$ , we have  $\sum_{t=1}^n |X_{m,t} - X_{m,t-1}|^2 \leq \frac{(B+K \log n)^2}{n}$ . As a result, applying Azuma-Hoeffding's inequality, we obtain

$$\mathbb{P}\left(|\mathcal{L}_m(\text{TF}) - \widehat{\mathcal{L}}_m(\text{TF})| \geq \tau\right) \leq 2e^{-\frac{n\tau^2}{2(B+K \log n)^2}}, \quad \forall m \in [M] \quad (10)$$

Let us consider  $Y_m := \mathcal{L}_m(\text{TF}) - \widehat{\mathcal{L}}_m(\text{TF})$  for  $m \in [M]$ . Then,  $(Y_m)_{m=1}^M$  are i.i.d. zero mean sub-Gaussian random variables. There exists an absolute constant  $c_1 > 0$  such that, the subgaussian norm, denoted by  $\|\cdot\|_{\psi_2}$ , obeys  $\|Y_m\|_{\psi_2}^2 < \frac{c_1(B+K \log n)^2}{n}$  via Proposition 2.5.2 of (Vershynin, 2018). Applying Hoeffding's inequality, we derive

$$\mathbb{P}\left(\left|\frac{1}{M} \sum_{m=1}^M Y_t\right| \geq \tau\right) \leq 2e^{-\frac{cnM\tau^2}{(B+K \log n)^2}} \implies \mathbb{P}(|\widehat{\mathcal{L}}(\text{TF}) - \mathcal{L}(\text{TF})| \geq \tau) \leq 2e^{-\frac{cnM\tau^2}{(B+K \log n)^2}}$$

where  $c > 0$  is an absolute constant. Therefore, we have that for any  $\text{TF} \in \text{Alg}$ , with probability at least  $1 - 2\delta$ ,

$$|\widehat{\mathcal{L}}(\text{TF}) - \mathcal{L}(\text{TF})| \leq (B + K \log n) \sqrt{\frac{\log(1/\delta)}{cnM}} \quad (11)$$

**Step 2: (Bound  $\sup_{\text{TF} \in \text{Alg}} |\mathcal{L}(\text{TF}) - \widehat{\mathcal{L}}(\text{TF})|$  where Alg is assumed to be a continuous search space).** Let

$$h(\text{TF}) := \mathcal{L}(\text{TF}) - \widehat{\mathcal{L}}(\text{TF})$$

and we aim to bound  $\sup_{\text{TF} \in \text{Alg}} |h(\text{TF})|$ . Following Definition C.3, for  $\varepsilon > 0$ , let  $\text{Alg}_\varepsilon$  be a minimal  $\varepsilon$ -cover of Alg in terms of distance metric  $\rho$ . Therefore,  $\text{Alg}_\varepsilon$  is a discrete set with cardinality  $|\text{Alg}_\varepsilon| := \mathcal{N}(\text{Alg}, \rho, \varepsilon)$ . Then, we have

$$\sup_{\text{TF} \in \text{Alg}} |\mathcal{L}(\text{TF}) - \widehat{\mathcal{L}}(\text{TF})| \leq \sup_{\text{TF} \in \text{Alg}'} \min_{\text{TF}' \in \text{Alg}_\varepsilon} |h(\text{TF}) - h(\text{TF}')| + \max_{\text{TF}' \in \text{Alg}_\varepsilon} |h(\text{TF}')|.$$

We will first bound the quantity  $\sup_{\text{TF} \in \text{Alg}'} \min_{\text{TF}' \in \text{Alg}_\varepsilon} |h(\text{TF}) - h(\text{TF}')|$ . We will utilize that loss function  $\ell(\cdot, \cdot)$  is  $C$ -Lipschitz. For any  $\text{TF} \in \text{Alg}$ , let  $\text{TF}' \in \text{Alg}_\varepsilon$  be its neighbor following Definition C.3. Then we can show that

$$\begin{aligned} & \left| \widehat{\mathcal{L}}(\text{TF}) - \widehat{\mathcal{L}}(\text{TF}') \right| \\ &= \left| \frac{1}{nM} \sum_{m=1}^M \sum_{t=1}^n (\ell(r_{mt}(a_{mt}), \text{TF}(\widehat{r}_{mt}(a_{mt})|\mathcal{H}_m^{t-1}, a_{mt})) - \ell(r_{mt}(a_{mt}), \text{TF}'(\widehat{r}_{mt}(a_{mt})|\mathcal{H}_m^{t-1}, a_{mt}))) \right| \\ &\leq \frac{L}{nM} \sum_{m=1}^M \sum_{t=1}^n \|\text{TF}(\widehat{r}_{mt}(a_{mt})|\mathcal{H}_m^{t-1}, a_{mt}) - \text{TF}'(\widehat{r}_{mt}(a_{mt})|\mathcal{H}_m^{t-1}, a_{mt})\|_{\ell_2} \\ &\leq L\varepsilon. \end{aligned}$$

Note that the above bound applies to all data-sequences, we also obtain that for any  $\text{TF} \in \text{Alg}$ ,

$$|\mathcal{L}(\text{TF}) - \mathcal{L}(\text{TF}')| \leq L\varepsilon.$$

Therefore we can show that,

$$\begin{aligned} & \sup_{\text{TF} \in \text{Alg}} \min_{\text{TF}' \in \text{Alg}_\varepsilon} |h(\text{TF}) - h(\text{TF}')| \\ &\leq \sup_{\text{TF} \in \text{Alg}} \min_{\text{TF}' \in \text{Alg}_\varepsilon} \left| \widehat{\mathcal{L}}(\text{TF}) - \widehat{\mathcal{L}}(\text{TF}') \right| + |\mathcal{L}(\text{TF}) - \mathcal{L}(\text{TF}')| \leq 2L\varepsilon. \quad (12) \end{aligned}$$

Next we bound the second term  $\max_{\text{TF}' \in \text{Alg}_\varepsilon} |h(\text{TF}')|$ . Applying union bound directly on  $\text{Alg}_\varepsilon$  and combining it with (11), then we will have that with probability at least  $1 - 2\delta$ ,

$$\max_{\text{TF}' \in \text{Alg}_\varepsilon} |h(\text{TF}')| \leq (B + K \log n) \sqrt{\frac{\log(\mathcal{N}(\text{Alg}, \rho, \varepsilon)/\delta)}{cnM}}$$

Combining the upper bound above with the perturbation bound (12), we obtain that

$$\max_{\text{TF} \in \text{Alg}} |h(\text{TF})| \leq 2C\varepsilon + (B + K \log n) \sqrt{\frac{\log(\mathcal{N}(\text{Alg}, \rho, \varepsilon)/\delta)}{cnM}}.$$

It follows then that

$$\mathcal{R}_{\text{MTL}}(\widehat{\text{TF}}) \leq 2 \sup_{\text{TF} \in \text{Alg}} |\mathcal{L}(\text{TF}) - \widehat{\mathcal{L}}(\text{TF})| \leq 4C\varepsilon + 2(B + K \log n) \sqrt{\frac{\log(\mathcal{N}(\text{Alg}, \rho, \varepsilon)/\delta)}{cnM}}$$

Again by setting  $\varepsilon = 1/\sqrt{nM}$

$$\mathcal{L}(\widehat{\text{TF}}) - \mathcal{L}(\text{TF}^*) \leq \frac{4C}{\sqrt{nM}} + 2(B + K \log n) \sqrt{\frac{\log(\mathcal{N}(\text{Alg}, \rho, \varepsilon)/\delta)}{cnM}}$$

The claim of the theorem follows.  $\square$

**Definition C.2.** (Covering number) Let  $Q$  be any hypothesis set and  $d(q, q') \geq 0$  be a distance metric over  $q, q' \in Q$ . Then,  $\bar{Q} = \{q_1, \dots, q_N\}$  is an  $\varepsilon$ -cover of  $Q$  with respect to  $d(\cdot, \cdot)$  if for any  $q \in Q$ , there exists  $q_i \in \bar{Q}$  such that  $d(q, q_i) \leq \varepsilon$ . The  $\varepsilon$ -covering number  $\mathcal{N}(Q, d, \varepsilon)$  is the cardinality of the minimal  $\varepsilon$ -cover.

**Definition C.3.** (Algorithm distance). Let  $\text{Alg}$  be an algorithm hypothesis set and  $\mathcal{H} = (a_t, r_t)_{t=1}^n$  be a sequence that is admissible for some task  $m \in [M]$ . For any pair  $\text{TF}, \text{TF}' \in \text{Alg}$ , define the distance metric  $\rho(\text{TF}, \text{TF}') := \sup_{\mathcal{H}} \frac{1}{n} \sum_{t=1}^n \|\text{TF}(\widehat{r}_t | \mathcal{H}^{t-1}, a_t) - \text{TF}'(\widehat{r}_t | \mathcal{H}^{t-1}, a_t)\|_{\ell_2}$ .

*Remark C.4. (Stability Factor)* The work of [Li et al. \[2023\]](#) also characterizes the stability factor  $K$  in Assumption 6.1 with respect to the transformer architecture. Assuming loss  $\ell(\cdot, \cdot)$  is  $C$ -Lipschitz, the algorithm induced by  $\text{TF}(\cdot)$  obeys the stability assumption with  $K = 2C((1 + \Gamma)e^\Gamma)^L$ , where the norm of the transformer weights are upper bounded by  $O(\Gamma)$  and there are  $L$ -layers of the transformer.

*Remark C.5. (Covering Number)* From Lemma 16 of [Lin et al. \[2023\]](#) we have the following upper bound on the covering number of the transformer class  $\text{TF}_\Theta$  as

$$\log(\mathcal{N}(\text{Alg}, \rho, \varepsilon)) \leq O(L^2 D^2 J)$$

where  $L$  is the total number of layers of the transformer and  $J$  and  $D$  denote the upper bound to the number of heads and hidden neurons in all the layers respectively. Note that this covering number holds for the specific class of transformer architecture discussed in section 2 of [\[Lin et al., 2023\]](#).

## C.2 Generalization Error to New Task

**Theorem C.6. (Transfer Risk)** Consider the setting of Theorem 6.2 and assume the source tasks are independently drawn from task distribution  $\mathcal{T}$ . Let  $\widehat{\text{TF}}$  be the empirical solution of (ERM) and  $g \sim \mathcal{T}$ . Then with probability at least  $1 - 2\delta$ , the expected excess transfer learning risk is bounded by

$$\mathbb{E}_g \left[ \mathcal{R}_g(\widehat{\text{TF}}) \right] \leq 4 \frac{C}{\sqrt{M}} + B \sqrt{\frac{2 \log(\mathcal{N}(\text{Alg}, \rho, \varepsilon)/\delta)}{M}}$$

where,  $\mathcal{N}(\text{Alg}, \rho, \varepsilon)$  is the covering number of transformer  $\widehat{\text{TF}}$ .

*Proof.* Let the target task  $g$  be sampled from  $\mathcal{T}$ , and the test set  $\mathcal{H}_g = \{a_t, r_t\}_{t=1}^n$ . Define empirical and population risks on  $g$  as  $\widehat{\mathcal{L}}_g(\text{TF}) = \frac{1}{n} \sum_{t=1}^n \ell(r_t(a_{mt}), \text{TF}(\widehat{r}_t(a_{mt}) | \mathcal{H}_g^{t-1}, a_t))$  and  $\mathcal{L}_g(\text{TF}) = \mathbb{E}_{\mathcal{H}_g} [\widehat{\mathcal{L}}_g(\text{TF})]$ . Again we drop  $\Theta$  from the transformer notation. Then the expected excess transfer risk following (ERM) is defined as

$$\mathbb{E}_g \left[ \mathcal{R}_g(\widehat{\text{TF}}) \right] = \mathbb{E}_{\mathcal{H}_g} \left[ \mathcal{L}_g(\widehat{\text{TF}}) \right] - \arg \min_{\text{TF} \in \text{Alg}} \mathbb{E}_{\mathcal{H}_g} [\mathcal{L}_g(\text{TF})]. \quad (13)$$

where  $\mathcal{A}$  is the set of all algorithms. The goal is to show a bound like this

$$\mathbb{E}_g \left[ \mathcal{R}_g(\widehat{\text{TF}}) \right] \leq \min_{\varepsilon \geq 0} \left\{ 4C\varepsilon + B \sqrt{\frac{2 \log(\mathcal{N}(\text{Alg}, \rho, \varepsilon)/\delta)}{T}} \right\}$$

where  $\mathcal{N}(\text{Alg}, \rho, \varepsilon)$  is the covering number.

**Step 1 ((Decomposition)):** Let  $\text{TF}^* = \arg \min_{\text{TF} \in \text{Alg}} \mathbb{E}_g [\mathcal{L}_g(\text{TF})]$ . The expected transfer learning excess test risk of given algorithm  $\widehat{\text{TF}} \in \text{Alg}$  is formulated as

$$\widehat{\mathcal{L}}_m(\text{TF}) := \frac{1}{n} \sum_{t=1}^n \ell(r_{mt}(a_{mt}), \text{TF}(\widehat{r}_{mt}(a_{mt}) | \mathcal{D}_m^{t-1}, a_{mt})), \quad \text{and}$$

$$\mathcal{L}_m(\text{TF}) := \mathbb{E}_{\mathcal{H}_m} \left[ \widehat{\mathcal{L}}_m(\text{TF}) \right] = \mathbb{E}_{\mathcal{H}_m} \left[ \frac{1}{n} \sum_{t=1}^n \ell(r_{mt}(a_{mt}), \text{TF}(\widehat{r}_{mt}(a_{mt}) | \mathcal{D}_m^{t-1}, a_{mt})) \right], \quad \forall m \in [M].$$

Then we can decompose the risk as

$$\begin{aligned} \mathbb{E}_g \left[ \mathcal{R}_g(\widehat{\text{TF}}) \right] &= \mathbb{E}_g \left[ \mathcal{L}_g(\widehat{\text{TF}}) \right] - \mathbb{E}_g \left[ \mathcal{L}_g(\text{TF}^*) \right] \\ &= \underbrace{\mathbb{E}_g \left[ \mathcal{L}_g(\widehat{\text{TF}}) \right] - \widehat{\mathcal{L}}_{\mathcal{H}_{\text{all}}}(\widehat{\text{TF}})}_a + \underbrace{\widehat{\mathcal{L}}_{\mathcal{H}_{\text{all}}}(\widehat{\text{TF}}) - \widehat{\mathcal{L}}_{\mathcal{H}_{\text{all}}}(\text{TF}^*)}_b + \underbrace{\widehat{\mathcal{L}}_{\mathcal{H}_{\text{all}}}(\text{TF}^*) - \mathbb{E}_g \left[ \mathcal{L}_g(\text{TF}^*) \right]}_c. \end{aligned}$$

Here since  $\widehat{\text{TF}}$  is the minimizer of training risk,  $b < 0$ . Then we obtain

$$\mathbb{E}_g \left[ \mathcal{R}_g(\widehat{\text{TF}}) \right] \leq 2 \sup_{\text{TF} \in \text{Alg}} \left| \mathbb{E}_g \left[ \mathcal{L}_g(\text{TF}) \right] - \frac{1}{M} \sum_{m=1}^M \widehat{\mathcal{L}}_m(\text{TF}) \right|. \quad (14)$$

**Step 2 (Bounding (14))** For any  $\text{TF} \in \text{Alg}$ , let  $X_t = \widehat{\mathcal{L}}_t(\text{TF})$  and we observe that

$$\mathbb{E}_{m \sim \mathcal{T}} [X_t] = \mathbb{E}_{m \sim \mathcal{T}} \left[ \widehat{\mathcal{L}}_m(\text{TF}) \right] = \mathbb{E}_{m \sim \mathcal{T}} \left[ \mathcal{L}_m(\text{TF}) \right] = \mathbb{E}_g \left[ \mathcal{L}_g(\text{TF}) \right]$$

Since  $X_m, m \in [M]$  are independent, and  $0 \leq X_m \leq B$ , applying Hoeffding's inequality obeys

$$\mathbb{P} \left( \left| \mathbb{E}_g \left[ \mathcal{L}_g(\text{TF}) \right] - \frac{1}{M} \sum_{m=1}^M \widehat{\mathcal{L}}_m(\text{TF}) \right| \geq \tau \right) \leq 2e^{-\frac{2M\tau^2}{B^2}}.$$

Then with probability at least  $1 - 2\delta$ , we have that for any  $\text{TF} \in \text{Alg}$ ,

$$\left| \mathbb{E}_g \left[ \mathcal{L}_g(\text{TF}) \right] - \frac{1}{M} \sum_{m=1}^M \widehat{\mathcal{L}}_m(\text{TF}) \right| \leq B \sqrt{\frac{\log(1/\delta)}{2M}}. \quad (15)$$

Next, let  $\text{Alg}_\varepsilon$  be the minimal  $\varepsilon$ -cover of  $\text{Alg}$  following Definition C.2, which implies that for any task  $g \sim \mathcal{T}$ , and any  $\text{TF} \in \text{Alg}$ , there exists  $\text{TF}' \in \text{Alg}_\varepsilon$

$$\left| \mathcal{L}_g(\text{TF}) - \mathcal{L}_g(\text{TF}') \right|, \left| \widehat{\mathcal{L}}_g(\text{TF}) - \widehat{\mathcal{L}}_g(\text{TF}') \right| \leq C\varepsilon. \quad (16)$$

Since the distance metric following Definition 3.4 is defined by the worst-case datasets, then there exists  $\text{TF}' \in \text{Alg}_\varepsilon$  such that

$$\left| \mathbb{E}_g \left[ \mathcal{L}_g(\text{TF}) \right] - \frac{1}{M} \sum_{m=1}^M \widehat{\mathcal{L}}_m(\text{TF}) \right| \leq 2C\varepsilon.$$

Let  $\mathcal{N}(\text{Alg}, \rho, \varepsilon) = |\text{Alg}_\varepsilon|$  be the  $\varepsilon$ -covering number. Combining the above inequalities ((14), (15), and (16)), and applying union bound, we have that with probability at least  $1 - 2\delta$ ,

$$\mathbb{E}_g \left[ \mathcal{R}_g(\widehat{\text{TF}}) \right] \leq \min_{\varepsilon \geq 0} \left\{ 4C\varepsilon + B \sqrt{\frac{2 \log(\mathcal{N}(\text{Alg}, \rho, \varepsilon)/\delta)}{M}} \right\}$$

Again by setting  $\varepsilon = 1/\sqrt{M}$

$$\mathcal{L}(\widehat{\text{TF}}) - \mathcal{L}(\text{TF}^*) \leq \frac{4C}{\sqrt{M}} + 2B \sqrt{\frac{\log(\mathcal{N}(\text{Alg}, \rho, \varepsilon)/\delta)}{cM}}$$

The claim of the theorem follows.  $\square$

*Remark C.7.* (Dependence on  $n$ ) In this remark, we briefly discuss why the expected excess risk for target task  $\mathcal{T}$  does not depend on samples  $n$ . The work of Li et al. [2023] pointed out that the MTL pretraining process identifies a favorable algorithm that lies in the span of the  $M$  source tasks. This is termed as inductive bias (see section 4 of Li et al. [2023]) [Soudry et al., 2018, Neyshabur et al., 2017]. Such bias would explain the lack of dependence of the expected excess transfer risk on  $n$  during transfer learning. This is because given a target task  $g \sim \mathcal{T}$ , the TF can use the learnt favorable algorithm to conduct a discrete search over span of the  $M$  source tasks and return the source task that best fits the new target task. Due to the discrete search space over the span of  $M$  source tasks, it is not hard to see that, we need  $n \propto \log(M)$  samples (which is guaranteed by the  $M$  source tasks) rather than  $n \propto d$  (for the linear setting).

### C.3 Table of Notations

Notations	Definition
$M$	Total number of tasks
$d$	Dimension of the feature
$\mathcal{A}_m$	Action set of the $m$ -th task
$\mathcal{X}_m$	Feature space of $m$ -th task
$M_{\text{test}}$	Tasks for testing
$M_{\text{pre}}$	Total Tasks for pretraining
$\mathbf{x}(m, a)$	Feature of action $a$ in task $m$
$\theta_{m,*}$	Hidden parameter for the task $m$
$\mathcal{T}_{\text{pre}}$	Pretraining distribution on tasks
$\mathcal{T}_{\text{test}}$	Testing distribution on tasks
$n$	Total horizon for each task $m$
$\mathcal{H}_m = \{I_t, r_t\}_{t=1}^n$	Dataset sampled for the $m$ -th task containing $n$ samples
$\mathcal{H}_m^t = \{I_s, r_s\}_{s=1}^t$	Dataset sampled for the $m$ -th task containing samples from round $s = 1$ to $t$
$\mathbf{w}$	Transformer model parameter
$\text{TF}_{\mathbf{w}}$	Transformer with model parameter $\mathbf{w}$
$\mathcal{D}_{\text{pre}}$	Pretraining in-context distribution
$\mathcal{H}_{\text{train}}$	Training in-context dataset
$\mathcal{D}_{\text{test}}$	Testing in-context distribution

Table 1: Table of Notations